COOPERATIVE RESEARCH CENTRE FOR **CATCHMENT HYDROLOGY**

OPTICAL PROPERTIES OF LEAVES IN THE VISIBLE AND NEAR-INFRARED UNDER BEAM AND DIFFUSE RADIANCE

TECHNICAL REPORT
Report 02/3
April 2002

Iain Hume / Tim McVicar / Michael Roderick

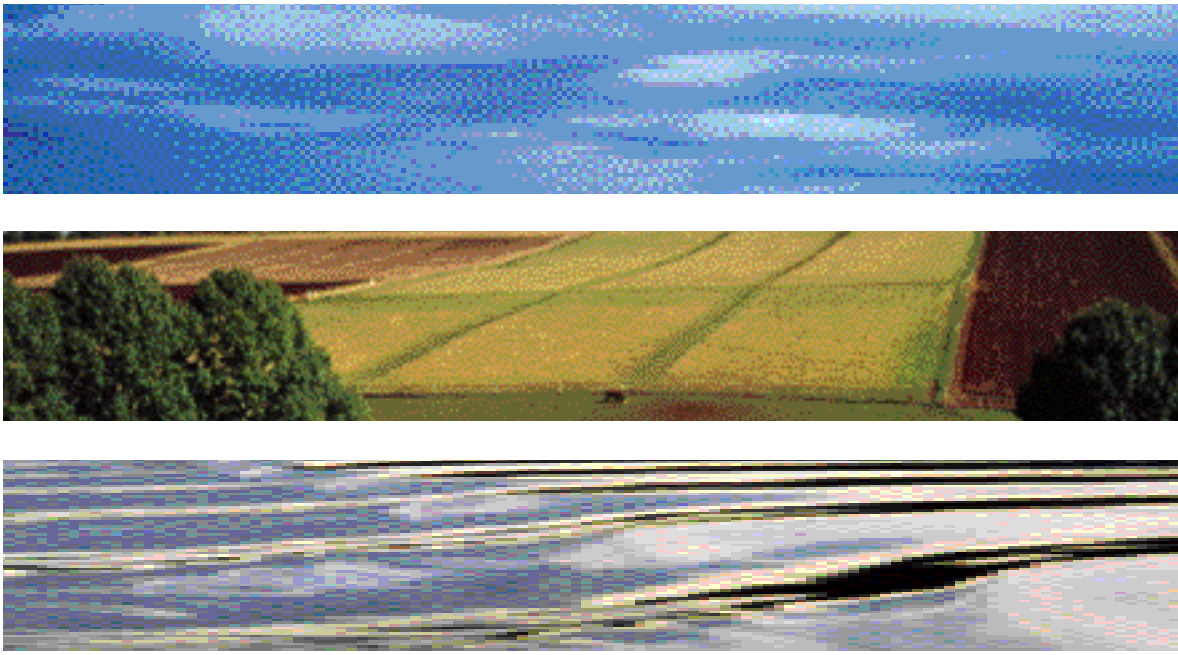

COOPERATIVE RESEARCH CENTRE FOR
CATCHMENT HYDROLOGY

Hume, I. H.

Optical Properties Of Leaves in the Visible and Near-Infrared Under Beam and Diffuse Radiance

Bibliography

ISBN 1 876006 85 4

1. Leaves - Optical properties. 2. Visibility. I. McVicar, Tim R. II. Roderick, Michael L. III. Cooperative Research Centre for Catchment Hydrology. IV. Title. (Series: Report (Cooperative Research Centre for Catchment Hydrology); 02/3)

581.48

Keywords

Leaves (of Plants)
Optical Properties
Light
Infrared Analysis
Diffusion
Remote Sensing
Satellite Imagery
Reflection
Shade
Habitat
Vegetation
Radiometry
Instrumentation
Landsat
AVHRR

Optical Properties of Leaves in the Visible and Near-Infrared Under Beam and Diffuse Radiance

Iain Hume[1,2,3], Tim McVicar[1], and Michael Roderick[2]

Technical Report 02/3
April 2002

1 CSIRO Land and Water, P.O. Box 1666, Canberra 2601, Australia
2 Ecosystems Dynamics Group, Research School of Biological Sciences, The Australian National University, Canberra, Australia
3 Cooperative Research Centre for Catchment Hydrology, P.O. Box 1666, Canberra 2601, Australia

Foreword

Around 5% of Australia is classified as woodland, ranging from 5-30% tree cover.

Important rural production takes place in woodlands. For example the pastoral industry occupies a large portion of Queensland's 222,000 km^2 of woodland. These regions must be managed to maintain their resource base while being profitable. It is important to control the number of grazing animals; the quantity of understorey feed available is a vital, but imprecise, piece of information used in this decision. Land-use impacts on the water balance and regional hydrology through vegetation. Agricultural and natural resource managers therefore need to know the amount of understorey and overstorey vegetation in these woodlands. Remote sensing has a role in this assessment.

This report describes laboratory studies to determine if the remote sensing signature of tree and grass leaves differ enough to allow them to be identified using broad-band satellite data. Additionally, further understanding of the way understorey and overstorey leaves absorb diffuse and beam light has been developed; the results provide an avenue forward for remote sensing in this difficult area.

This research was part of a larger project funded in part by the Land and Water Australia Climate Variability in Agriculture Program. The research partners were the Cooperative Research Centre for Catchment Hydrology, CSIRO Land and Water, CSIRO Earth Observation Centre, CSIRO Atmospheric Research, the Bureau of Rural Sciences, the Australian National University and Queensland Natural Resources and Mines.

Dr Rob Vertessy
Deputy Director
CRC for Catchment Hydrology

Acknowledgements

Iain Hume is a PhD scholar funded by the Cooperative Research Centre for Catchment Hydrology. This research is part of that study. Without extra funding from the Land and Water Australia's (LWA) Climate Variability in Agriculture Program, and the encouragement of Dr Barry White (LWA) and Greg Laughlin of the Bureau of Rural Sciences, this work would not have been possible. Bruce Evans, of Bartondale Marine, fashioned the goniometer from our rough sketches and even rougher ideas. We are especially grateful to Paul Daniel of CSIRO Land and Water who was a constant source of constructive criticism and "black hat thinking" during the evolution of diffuse light balance methods. Lastly we are grateful to Dr Edward King of the CSIRO Earth Observation Centre for his constructive review of this manuscript.

Abstract

Methods and equipment were developed to measure the directional transmittance and hemispherical reflectance and transmittance of diffuse light. The hemispherical reflectance (ρ), absorptance (α) and transmittance (τ) of both beam and diffuse light by dicot and monocot leaves of varying thicknesses was estimated. Measurements were made at 1 nm increments in the visible and near-infrared (NIR) parts of the spectrum (350-2500 nm).

Transmittance of diffuse light was anisotropic with more light transmitted at angles close to the leaf surface normal. We found both dicot and monocot leaves exhibited this focusing of diffuse light. Dicot leaves transmitted a greater proportion of red and NIR light than monocot leaves at incidence angles up to 60^o from the leaf normal. However, there were no differences in the hemispherical transmittance of dicot and moncot leaves.

The hemispherical reflectance of beam and diffuse light was almost identical at all wavelengths. Leaf thickness had minimal effect on the ρ, τ, and α. The reflectance of beam near-infrared light by grass or tree leaves was statistically the same (P = 0.05). We conclude then that tree and understory leaves cannot be distinguished by their remotely sensed broad-band reflectance.

At visible wavelengths the optical properties of leaves were the same under either beam and diffuse illumination, with most light (c. 85%) being absorbed. However, in the near-infrared, the optical properties depended on whether the incident light was beam or diffuse. The reflection of beam and diffuse near-infrared light were similar (c. 5%), but the absorption of diffuse light was much higher (23%) than of beam light (5%). This finding is consistent with the strong angular dependence of leaf optical properties in the near-infrared. The result has important implications for modelling the energy balance of plant canopies.

List of Figures

List of Tables

1. Introduction

As a general rule, areas of woody vegetation, such as forests and woodlands, usually appear darker than grasslands and croplands in remotely sensed images (Fiorella and Ripple, 1993, Brondizio et al., 1996, Steininger, 1996, Matherson and Ringrose, 1994, McCloy and Hall, 1991). Assuming (near) full vegetation cover, it follows that this gross difference could be largely explained by either; (a) the leaves of woody plants reflecting less light, and/or (b) a larger amount of shaded surface in woody vegetation visible to satellite instruments.

No general trend has emerged of differences in reflectance between tree and grass leaves (McCloy and Hall, 1991, Asner, 1998). Knapp and Carter (1998) found no consistent pattern in the reflectance and transmittance of beam near-infrared (NIR) light by leaves of 26 species with habitat; their leaves were from open, intermediate and shaded understory habitats. Leaf optical properties showed trends with leaf thickness, but the high variance of leaf thickness within habitats prevented the use of these properties to identify a leaf's habitat of origin. In summary, there is not a consistent body of evidence suggesting that there are generic trends in leaf optical properties with habitat.

By way of contrast, the second explanation suggested above appears to be more promising. For example, observations show that variations in fraction of shade viewed by the sensor is a major source of variation in remotely sensed data acquired over forested landscapes (Hall et al., 1995). Further, modelling studies suggest that much of the variation in bulk surface reflectance, particularly in the near-infrared part of the spectrum, is most likely caused by variations in the geometric arrangement of leaves within the canopy (Asner, 1998), rather than the optical properties of those leaves.

Smith et al. (1997) proposed that leaves evolve to optimise the gradients of light and CO_2 within them. Understory (monocot) leaves lack the palisade mesophyll of overstory (dicot) leaves. This fundamental structural difference has been shown to result in deeper penetration of beam light in dicots, but equivalent penetration of diffuse light in both dicots and monocots (Vogelmann and Martin, 1993). Both canopy structure and productivity are known to be very sensitive to changes in the amount of diffuse light (Roderick et al., 2001) and we speculate that the optical properties of leaves may be different under conditions of diffuse illumination.

The aim of this study was to assess whether there were consistent differences in the optical properties of overstory and understory leaves. We tested these differences in the visible and near-infrared parts of the spectrum under conditions of beam and diffuse illumination. To make these investigations, we had to develop methods and construct new equipment because, as far as we are aware, there are no commercially available instruments which can be used to estimate the directional transmittance and hemispherical reflectance and transmittance of leaves irradiated with diffuse light. We used these new methods, together with the well known traditional approaches developed for use with beam light, to measure the optical properties of various tree (dicot) and understory (monocot) leaves of varying thickness.

Measurements of high temporal density are needed to detect change in vegetation. Satellite remote sensing instruments with this characteristic have relatively few, but ecological significant, broad spectral bands [Landsat Thematic Mapper (TM); National Oceanic and Atmospheric and Administration (NOAA); Advanced Very High Resolution Radiometer (AVHRR)]. To assess the ability of these instruments to discriminate between dicot and monocot leaves, we evaluated leaf optical properties in Landsat and AVHRR spectral bands.

Table 1 gives explanations of the symbols used in this report.

Table 1. Description of symbols used in the text.

Symbol	Description	Units
A_s	Internal surface area of an integrating sphere	cm^2
ϕ_i	Light flux illuminating an integrating sphere	W
F	Fraction of the area of an integrating sphere wall occupied by ports	None
f_i	Fraction of the area of an integrating sphere wall occupied by the i^{th} port	None
I_{00}	Spectral radiance measured from zenith ($\theta = 0$)	$^{\#}$DN nm^{-1}
$I_{\theta\phi}$	Spectral radiance measured from θ and ϕ	DN nm^{-1}
$I_{n\theta\phi}$	Directional spectral radiance measured from θ and ϕ normalised to that measured form the zenith ($I_{\theta\phi}/I_{00}$)	DN nm^{-1}
I_{e00}	Directional spectral radiance of the empty goniometer measured from zenith ($\theta = 0$)	DN nm^{-1}
$I_{e\theta\phi}$	Directional spectral radiance of the empty goniometer measured from θ and ϕ	DN nm^{-1}
$I_{en\theta\phi}$	Directional spectral radiance of the empty goniometer measured from θ and ϕ normalised to that at zenith ($I_{\theta\phi}/I_{00}$)	DN nm^{-1}
$I_{l\theta\phi}$	Directional spectral radiance of a leaf measured from θ and ϕ	DN nm^{-1}
L_r	Spectral radiance of an integrating sphere containing reference material	DN nm^{-1}
L_s	Spectral radiance of an integrating sphere containing sample	DN nm^{-1}
L_{std}	Spectral radiance of a comparison integrating sphere while illuminating the reference material with the sample port empty	DN nm^{-1}
L_{samp}	Spectral radiance of a comparison integrating sphere while illuminating the reference material with a sample in the port	DN nm^{-1}
M	Integrating sphere multiplier	None
n	The number of ports in an integrating sphere	None
z	Leaf thickness	μm
α	Spectral absorbance factor	None
α_{rb}	Absorbance of beam light in red wavebands	None
α_{nirb}	Absorbance of beam light in near-infrared wavebands	None
ϕ	Azimuth angle between the leaf axis and the direction from which a measurement was made	°
θ	Zenith angle between the leaf normal and the direction from which a measurement was made	°
ρ	Spectral reflectance factor	None
ρ_r	Spectral reflectance factor of a standard material	None
ρ_s	Spectral reflectance factor of a sample	None
ρ_w	Spectral reflectance of an integrating sphere wall	None
$\bar{\rho}_s$	Average spectral reflectance of a substitution integrating sphere with a sample in place	None

$\overline{\rho}_r$	Average spectral reflectance of a substitution integrating sphere with the reference material in place	None
$\overline{\rho}$	Average spectral reflectance factor of an integrating sphere	None
$\overline{\rho}_{\text{std}}$	Average spectral reflectance of an comparison integrating sphere while illuminating the standard	None
$\overline{\rho}_{\text{samp}}$	Average spectral reflectance of an comparison integrating sphere while illuminating the standard	None
$\rho_{0:h}$	Hemispherical spectral reflectance of beam irradiance	None
$\rho_{h:h}$	Hemispherical spectral reflectance of diffuse irradiance	None
ρ_i	Spectral reflectance factor of the i^{th} port of an integrating sphere	None
ρ_{rb}	Spectral Reflectance of beam light in red wavebands	None
ρ_{nirb}	Spectral reflectance of beam light in near-infrared wavebands	None
ρ_{rd}	Reflectance of diffuse light in red wavebands	None
ρ_{nird}	Reflectance of diffuse light in near-infrared wavebands	None
τ	Spectral transmittance factor	None
τ_r	Spectral transmittance factor of a standard material	None
$\overline{\tau}_n$	Weighted mean hemispherical transmittance calculated by the Voglemann and Björn (1984) scheme	None
τ_{rel}	Spectral transmittance factor at θ relative that at zenith (θ=0)	None
τ_s	Spectral transmittance factor of a sample	None
$\tau_{0:h}$	Hemispherical spectral transmittance of beam irradiance	None
$\tau_{h:h}$	Hemispherical spectral transmittance of diffuse irradiance	None
$\tau_{h:0}$	Directional spectral transmittance measured from zenith of diffuse irradiance	None
$\tau_{n\theta\phi}$	Spectral transmittance of the empty satellite illuminating sphere measured from θ, ϕ normalized to then measured from zenith	None
$\tau_{l\theta\phi}$	Directional spectral transmittance of a leaf measured from θ and ϕ	None
τ_{rb}	Hemispherical transmittance of beam light in red wavebands	None
τ_{nirb}	Hemispherical transmittance of beam light in near-infrared wavebands	None
τ_{rd}	Hemispherical transmittance of diffuse light in red wavebands	None
τ_{nird}	Hemispherical transmittance of diffuse light in near-infrared wavebands	None

Note: # DN = spectroradiometer reading in digital numbers.

2. Methods

2.1 Introduction

Under beam irradiance, the hemispherical reflectance ($\rho_{o:h}$) and hemispherical transmittance ($\tau_{o:h}$) of leaves can both be measured directly with commercially available instruments. However, as far as we are aware, there are no instruments available to measure the hemispherical reflectance ($\rho_{h:h}$) or hemispherical transmittance ($\tau_{h:h}$) of leaves under diffuse irradiance. We measured $\rho_{h:h}$ by applying integrating sphere reflectance theory in a novel way that enabled the use of an available integrating sphere. It was necessary to characterise the reflective properties of the integrating sphere before it could be used in this way. To measure $\tau_{h:h}$ we had to: (1) construct an instrument to measure the directional nature of transmitted light; (2) measure the observing characteristics of the radiometer; and (3) apply a hemispherical weighting scheme to directional measurements of transmitted radiance.

In this section, the theory and use of integrating spheres are described. We begin in Section 2.2 by describing how integrating spheres are used to make the necessary measurements. Integrating sphere reflectance theory and its application to calculate the reflectance of diffuse light by leaves is explained in Section 2.3.

In order to apply integrating sphere theory the physical dimensions of a sphere and, most importantly, the reflectance of its wall must be known. We developed a way to estimate the sphere's average wall reflectance, described in Section 2.4.

Our equipment was only able to measure the light transmitted by leaves in one direction. A scheme and equipment to measure the directional distribution of radiance are described in Section 2.5.

The hemispherical irradiance of the surface of a hemisphere can be estimated from a number of samples of directional radiance over the hemisphere. Section 2.6 outlines a weighting scheme to do this and describes experiments to characterise the instruments used.

Using these techniques we then measured the leaf light balance of a number of dicot and moncot leaves. Section 2.7 gives details of the species used, the measurement procedure and data analysis protocol.

2.2 Integrating Sphere Configuration

Integrating spheres collect and angularly integrate radiant light flux. They trap the flux in all directions that either enters the sphere through a port or that is reflected from a sample placed within the sphere. Integrating spheres are most commonly used measure the total reflectance or transmittance of light. These measurements are almost always made as a function of wavelength (spectrally).

Transmittance is calculated by externally illuminating the sphere's sample port and first measuring the radiance of the sphere while the port is empty (**Figure 1a**) and then when the material under study is placed over the sphere's entrance port (**Figure 1b**). Reflectance is calculated by measuring the sphere's radiance while illuminating a reference material of known reflectance (**Figure 1c**) and the material of interest (**Figure 1d**). The sphere collects all specular and diffuse components of the transmitted or reflected radiance and these are termed the hemispherical transmittance ($\tau_{0:h}$) and the hemispherical reflectance ($\rho_{0:h}$).

The transmittance factor (τ), reflectance (ρ) or absorbance (α) are measured relative to that of the reference material and are expressed as factors in the range 0-1. Ideally the ratio of the sample reflectance factor (ρ_s) to the reference (ρ_r) equals the ratio of the radiance produced in the sphere by the sample material (L_s) to that produced by the standard (L_r), the radiance factor.

$$\frac{L_s}{L_r} = \frac{\rho_s}{\rho_r} \tag{1}$$

Normally the transmittance standard is measured before the sample is placed across the entrance port (**Figure 1a**). Calibration to a reflectance standard is achieved by substituting the sample with a standard reference material of known reflectance factor (ρ_r) (**Figure 1c**). This substitution of materials results in a change in the average reflectance in the sphere wall ($\overline{\rho}$) that complicates the relationship between L_s and L_r. The true relationship is:

$$\frac{L_s}{L_r} = \frac{\rho_s}{\rho_r} \cdot \frac{1-\overline{\rho}_r}{1-\overline{\rho}_s} \tag{2}$$

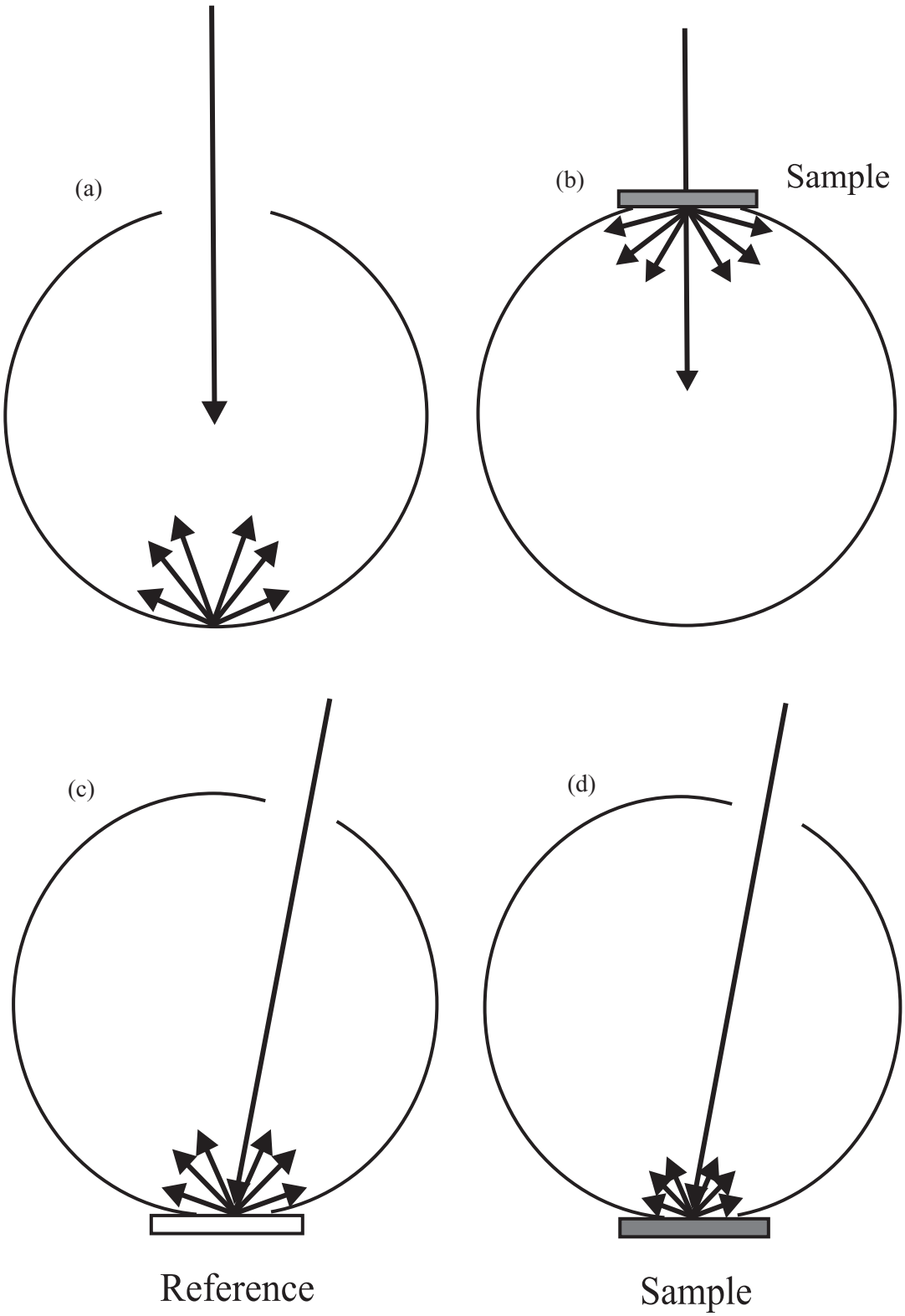

Figure 1. A substitution integrating sphere configured to measure (a) the radiance of the transmittance reference, (b) the transmitted radiance of the sample, (c) the radiance of the reflectance reference and (d) the reflected radiance of the sample.

The average reflectance of the sphere wall ($\overline{\rho}_s$) cannot be determined since it also depends on ρ_s. Average sphere wall reflectance can be kept constant by mounting both sample and reference simultaneously into ports in the sphere, termed a comparison sphere. In this configuration a single beam of light alternately illuminates the reference material and the sample (**Figure 2a**). **Equation 1** can be applied directly to measurements made with a comparison sphere. The average wall reflectance of the simple substitution sphere also changes when the transmittance sample is introduced (Compare **Figures 1a and 1b**). For this reason transmittance should also be measured in a comparison sphere (**Figure 2b**). The LICOR 1800-12 integrating sphere used in this experiment is a comparison sphere permitting use of **Equation 1**.

So far we have only considered the reflection or transmission of a directional beam of light. The directional reflectance and transmittance of diffuse light can be measured using a substitution integrating sphere with an internal light source (**Figures 3a and 3b**). Once again the quantity measured is termed a 'radiance factor' since the radiance of the sample is compared with the radiance of a reference material. To collect all the light reflected or transmitted in the configurations shown in **Figures 3a and 3b** requires an auxiliary sphere to be mounted on the exit port of the substitution sphere. This apparatus is often not available and an alternative is to employ the change in sphere wall reflectance caused by introducing a sample to the sphere. A substitution integrating sphere can be configured to make these measurements (**Figures 3c**

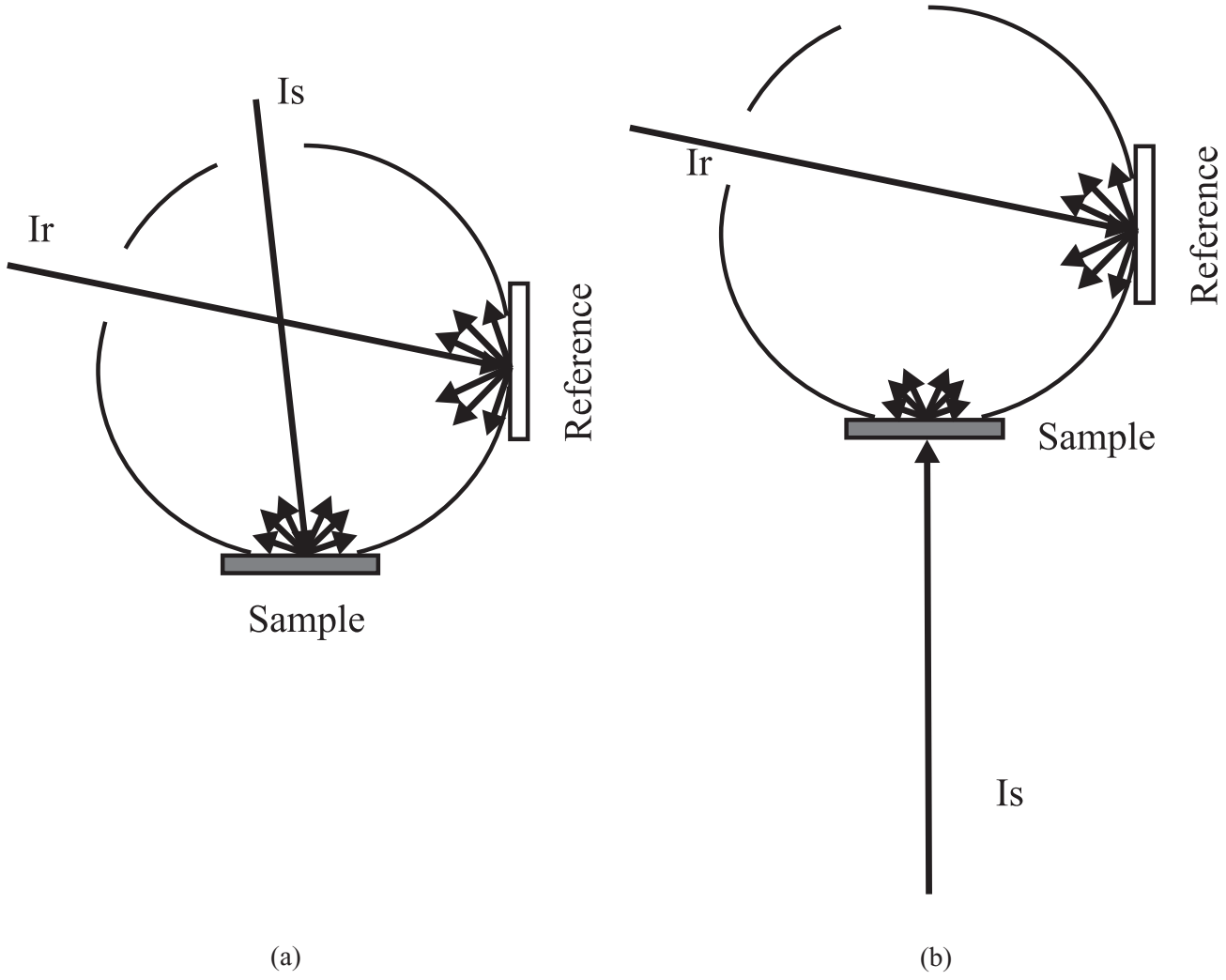

Figure 2. A comparison integrating sphere showing the measurement of (a) reflectance and (b) transmittance. The illuminating light beam is directed at the reference material (Ir) to make the reference measurement and at the sample (Is) to make the sample measurement.

and 3d). When the sample is introduced the average reflectance of the sphere wall increases which in turn increases the radiance from the sphere. Knowing this increase in sphere radiance, together with the surface area of the sphere not occupied by ports and the surface area of the port containing the sample, the reflectance of the sample can be found by solving the radiance equation for the sphere (see Section 2.3).

The directional transmission of diffuse light measured by a comparison integrating sphere (**Figure 3b**) can be used to estimate the hemispherical transmittance of that light by applying the methods of Section 2.5.

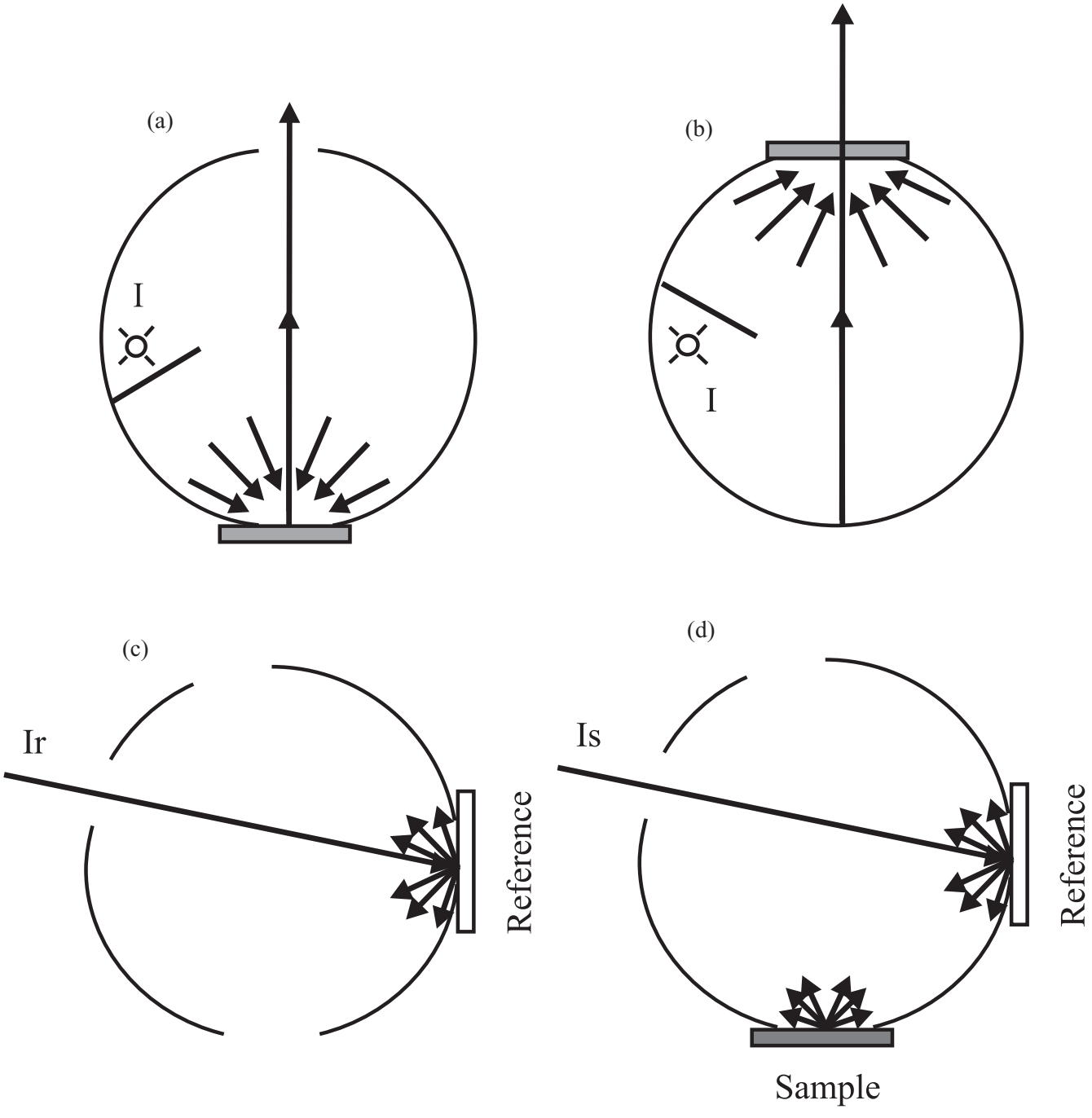

Figure 3. An internally illuminated substitution integrating sphere configured to measure (a) reflectance and (b) transmittance to calculate hemispherical:directional reflectance and transmittance factors. A comparison integrating sphere configured to measure the hemispherical:hemispherical radiance of (c) a reference material and (d) a sample.

2.3 Integrating Sphere Theory

The radiance (L_s) of an integrating sphere of internal surface area A_s illuminated by a light source of flux ϕ_i is given by (Labsphere, 1999):

$$L_s = \frac{\phi_i}{\pi A_s} M \tag{3}$$

Where ρ is the reflectance of the sphere wall, which is assumed constant, and ϕ is the fraction of the surface area of the sphere wall that is occupied by ports. M is known as the "multiplier" of the sphere and depends on the sphere's dimensions and configuration. The general form of M for a sphere with n ports is:

$$M = \frac{\rho_0}{1 - \left[\rho_w \left(1 - \sum_{i=o}^{n} f_i \right) + \sum_{i=o}^{n} \rho_i f_i \right]} \tag{4}$$

where; ρ_0 = the initial reflectance of the incident flux off the reference material

ρ_w = the reflectance of the sphere wall

ρ_i = the reflectance of the i[th] port

f_i = the fraction of the sphere surface area occupied by the i[th] port

The quantity $\rho_w \left(1 - \sum_{i=o}^{n} f_i \right) + \sum_{i=o}^{n} \rho_i f_i$ can be described as the average reflectance of the integrating sphere $\overline{\rho}$. Thus, the "multiplier" can be written in terms of the initial and average reflectance:

$$M = \frac{\rho_0}{1 - \overline{\rho}} \tag{5}$$

In our case the only port that can reflect light is the sample port; all other ports are non-reflective. When the sample port is empty (**Figure 3c**) the average wall reflectance $\overline{\rho}_{std}$ is:

$$\overline{\rho}_{std} = \rho_w (1 - f) \tag{6}$$

When a sample is placed in the sample port (**Figure 3d**) the average reflectance of the sphere $\overline{\rho}_{samp}$ is increased by the contribution from the sample ($\rho_{smp} f_{smp}$):

$$\overline{\rho}_{smp} = \rho_w \left(1 - \sum_{i=o}^{n} f_i \right) + \rho_{smp} f_{smp} \tag{7}$$

To find the unknown reflectance ρ_{smp} we can divide L_{std} by L_{smp} as follows:

$$\frac{L_{std}}{L_{smp}} = \frac{\dfrac{\rho_0}{1 - \rho_w (1 - f)}}{\dfrac{\rho_0}{1 - \rho_w \left(1 - \sum_{i=o}^{n} f_i \right) - \rho_{smp} f_{smp}}} \tag{8}$$

Thus, assuming that $\rho_0 = \rho_w$, **Equation 8** can be solved for ρ_{smp} as:

$$\rho_{smp} = -\frac{1}{f_{smp}} \left\{ \frac{L_{std} \left[1 - \rho_w (1 - f) \right]}{L_{smp}} - 1 + \rho_w (1 - f) \right\} \tag{9}$$

2.4 Sphere Characterisation

The solution of **Equation 9** assumes knowledge of the reflectance of the sphere wall, but this was unknown for the LICOR 1800-12 (LI-COR, 1984) integrating sphere used in this experiment. The sphere wall spectral reflectance was estimated with an 'optimisation' experiment in which the sphere radiance was measured in 1 nm intervals over the range 350 - 2500 nm with an ASD FR spectroradiometer (ASD, 1999). L_{std} was measured by illuminating the sphere's internal pressed barium-sulphate reference standard while the sample port was empty. L_{smp} was measured by illuminating the internal pressed barium-sulphate standard while a spectralon SRM-990 panel of known hemispherical reflectance (Labsphere, 1997) was in the sample port. The sample reflectance was calculated by **Equation 9** at the 22 wavelengths at which the spectralon's reflectance was known. At each of these wavelengths

the wall reflectance (ρ_w) was varied from 0.97 to 0.99 in steps of 0.001 and the ρ_w that minimised the difference between the estimated and known sample reflectance was ascribed to that wavelength. The spectral wall reflectance at 1 nm intervals between 350 and 1500 nm was summarised using a spline function available in the IDL™ software package (**Figure 4**). This smoothed spectral reflectance factor of the LICOR integrating sphere was used for all subsequent calculations.

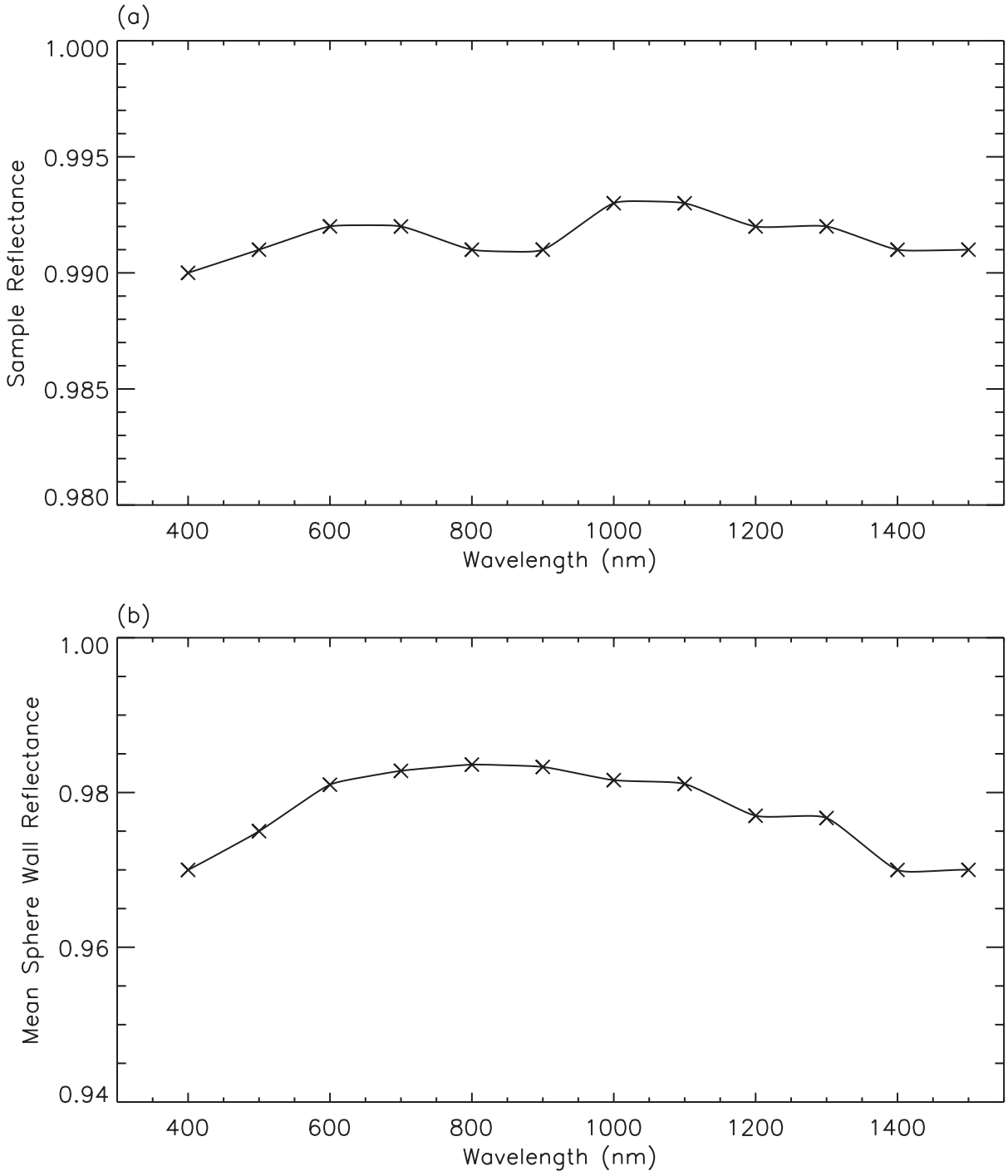

Figure 4. Estimation of mean sphere wall reflectance. (a) the calibrated reflectance of the spectralon 990 panel (X) and that resulting from optimizing Eqn. (8) smoothed to 1nm intervals —— using a spline function available in the IDL™ software package with the "tension" of the spline set to 10 to ensure a smooth fit through the 20 measured data points. (b) the optimal mean reflectance of the Licor 1800-12 integrating sphere wall that resulting from the optimization at points (+) smoothed to 1nm intervals (———).

2.5 Measurement of Directional Radiance.

A goniometer was constructed to measure the directional spectral radiance. A Labsphere® satellite illuminating sphere (SIS) mounted in the goniometer was used as a source of diffuse light (**Plate 1**). The SIS was illuminated internally by a 10 W halogen lamp that was shielded to prevent direct illumination of the sphere exit port. The direction of each radiance measurement was specified by the zenith angle relative to the leaf normal (θ) and azimuth angle relative to the leaf axis (ϕ).

2.5.1 Satellite illuminating sphere radiance characteristics

We first characterised the directionality of the radiance of the SIS sphere before measuring the directional transmittance of leaves. Sphere radiance was measured without a leaf mounted in the exit port in seven 15° increments of zenith angle (θ) from 0° to 75° and seven 30° increments of azimuth angle (ϕ) from 0° to 180°. This suite of directional measurements was repeated five times.

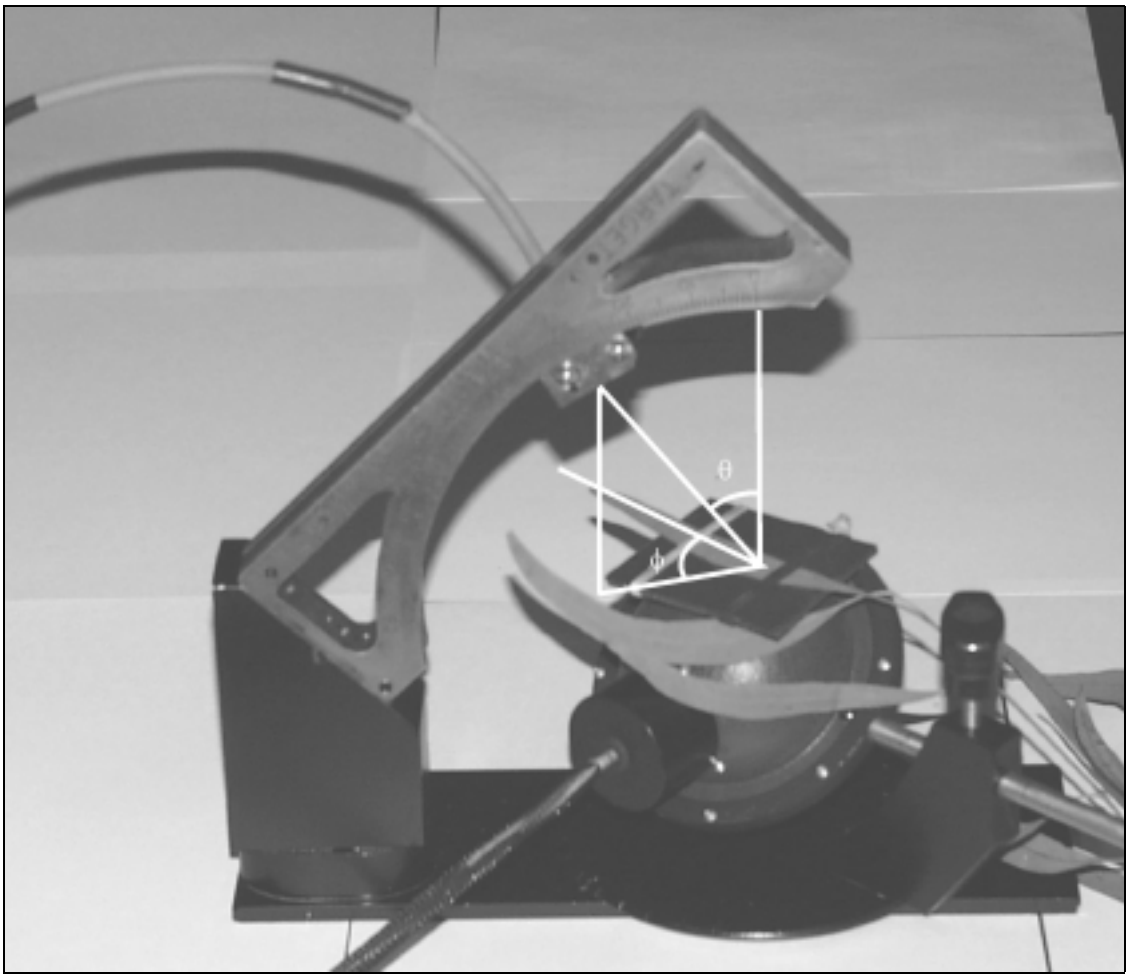

Plate 1. The goniometer showing a leaf mounted in the instrument. The spectroradiometer fiber optic probe points at the center of the center of the sphere exit port from all measurement positions. Radiance can be measured over a range of azimuth angles (ϕ) from 0° to 180° and zenith angles (θ) from 0° to 90°. The configuration shows the fiber optic is positioned to measure radiance at an azimuth angle of 45° and a zenith angle of 30°.

All radiance measurements were made with a Unispec spectroradiometer in the wavelength range 300-1000 nm. The spectroradiometer integration time was set to that which just prevented saturation of the instrument at leaf normal ($\theta = 0$). Ten spectra were sampled and averaged at each measurement location. Dark spectra, scanned with the instrument shutter closed and the fiber optic tip covered with a dark cloth, were taken before and after the measurements of sphere radiance. These determined the background radiance and the mean of these dark spectra was subtracted from the radiance spectra before analysis.

There was no clear effect of azimuth angle on the sphere radiance. However, when viewed from the 75° zenith angle the sensor's view of the sphere exit port was obstructed by the flange joining the two halves of the sphere; lowering radiance measured at azimuth angles more than 60° (**Figure 5**). The spectral balance of the sphere's radiance was unchanged with zenith angle, but the radiance was less at higher zenith angles (**Figure 6**). The seven directional radiance measurements at the same zenith angle in each waveband were averaged and normalised to the mean radiance measured at zenith ($\theta = 0$) and a strong linear relationship between the normalised radiance ($I_{n\theta}$) and θ was found.

$$I_{n\theta} = 1.13\cos\theta - 0.13 \qquad (10)$$

Each directional measurement of radiance was normalised to that measured at zenith by $I_{en\theta\phi} = I_{e\theta\phi}/I_{e00}$.

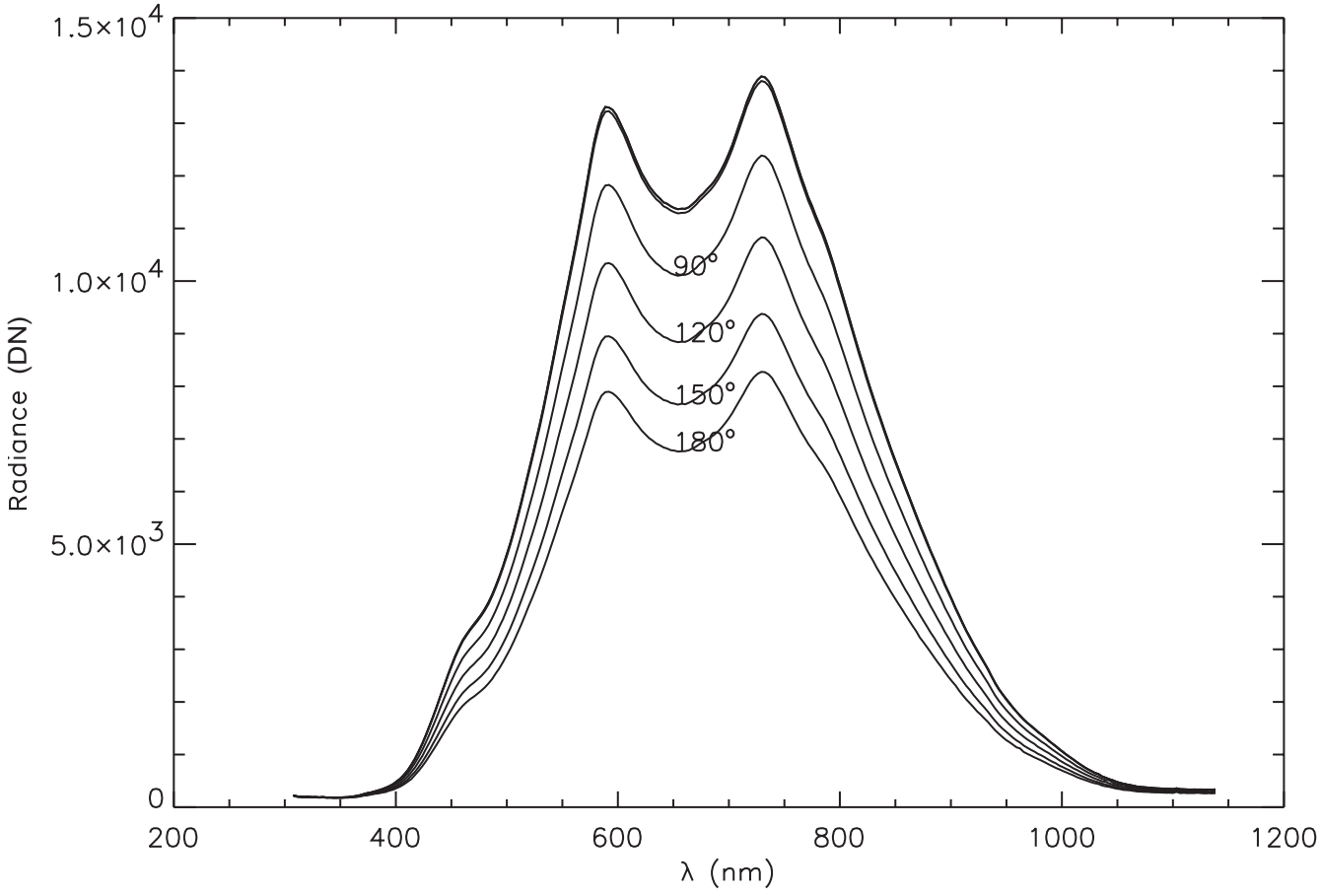

Figure 5. Observed radiance (DN) of the satellite illuminating sphere measured with a Unispec spectroradiometer at a zenith observation angle of 75° and azimuth angles between 0° to 180° (shown on the plot). (Note: the plots of spectral radiance at azimunth angles 0°, 30° and 60° overlay each other.)

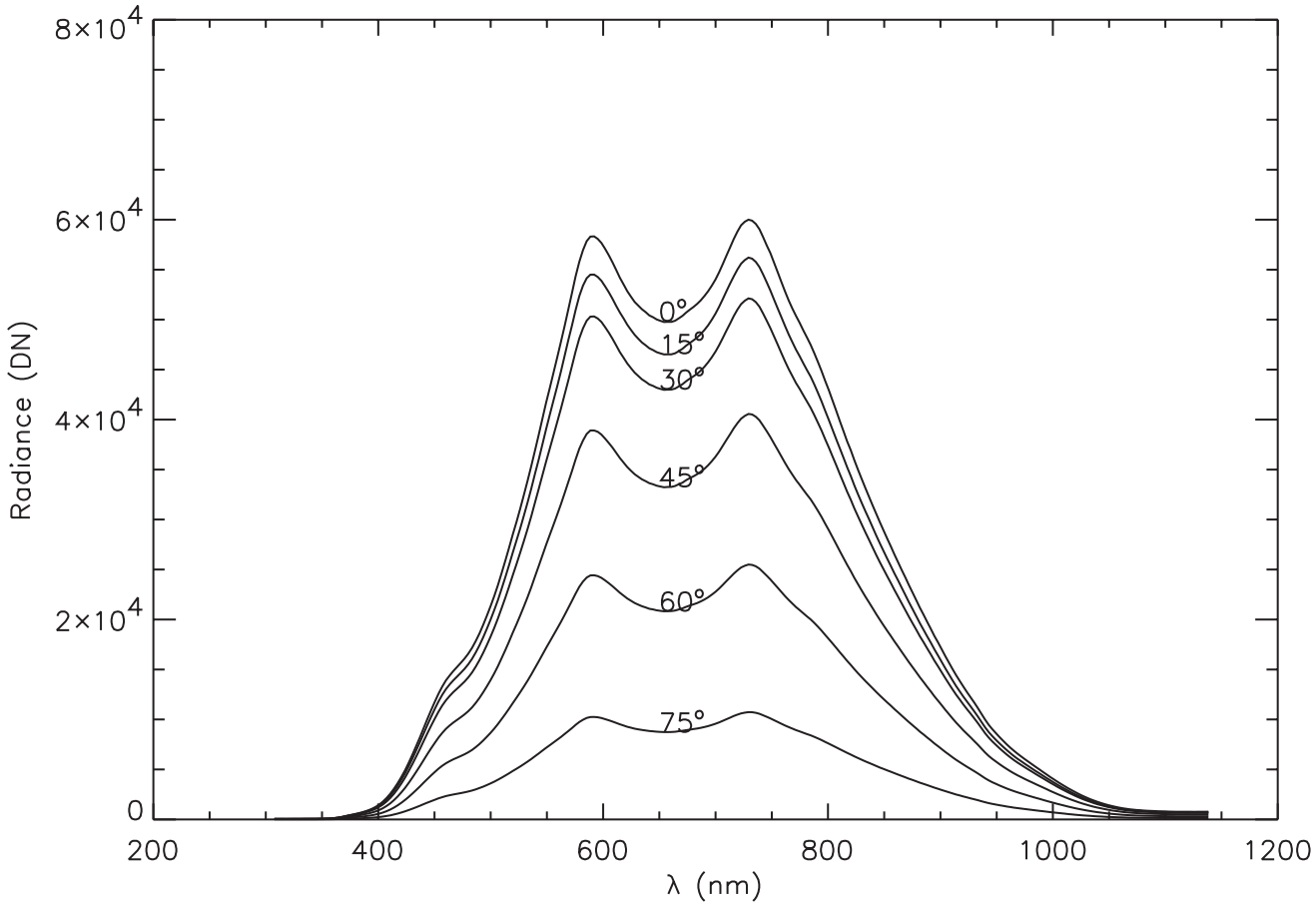

Figure 6. Observed radiance (DN) of the satellite illuminating sphere at zenith observation angles of 0°, 15°, 30°, 45°, 60°, and 75° (shown in the plot). The radiance plotted at each zenith angle is the mean of the seven measurements made at 30° increments in azimuth angles from 0° to 180°.

2.5.2 Patterns in the directional nature of transmittance of leaves

The directional transmittance of dicotyledenous tree leaves (*Eucalyptus maniflora*) and monocotyledous grass leaves (*Paspalum dilatatum*) was investigated. The radiance of leaves mounted in a leaf holder on the SIS was measured with a Unispec spectroradiometer from six θ (0, 15, 30, 45, 60, and 75°) at each of seven ϕ (0, 30, 60, 90, 120, 150 and 180°). Each spectrum was averaged over the red (580 - 680 nm) and near-infrared (725 - 1100 nm) wavebands to correspond with the bandwidths of the NOAA AVHRR instrument (Cracknell, 1997). The directional radiances ($I_{l\theta\phi}$) and transmittances ($\tau_{l\theta\phi}$) were calculated in these two bandwidths.

The SIS radiance was measured at zenith with no leaf in the holder (I_{e00}). The directional radiance at zenith angles away from the zenith ($I_{e\theta\phi}$) calculated by multiplying the zenith radiance by the normalised directional radiance ($I_{e\theta\phi} = I_{e00}$ x $I_{n\theta\phi}$). The directional transmittance was calculated as $\tau_{\theta\phi} = I_{l\theta\phi} / I_{e\theta\phi}$. We found for all leaves that at a given zenith angle neither the red nor near-infrared transmittance changed significantly with azimuth angle; the changes in zenith angle dominated any small effect of azimuth angle. Therefore, subsequent measurements of transmittance were made from a single azimuth of 45° while the θ was varied from 0° to 75° in five 15° increments ($\tau_{\theta,45}$).

2.5.3 Estimation of hemispherical transmittance using the LICOR integrating sphere

The configuration of the LICOR sphere (**Plate 2b**) allows only zenith measurement of the light transmitted by leaves when illuminated with diffuse light ($\tau_{h:0}$). To permit calculation of the hemispherical transmittance of diffuse light ($\tau_{h:h}$) the pattern of directional transmittance of leaves was measured by goniometry.

In this phase of the experiment all radiance measurements were made with the ASD FR spectroradiometer. Zenith radiance of the SIS with no leaf in the holder was measured (I_{e0}), the radiance at other zenith angles (θ), denoted $I_{e\theta,45}$ was estimated using **Equation 10**. The radiance of the SIS with a leaf in the holder was measured at θ = 0, 15, 30, 45, 60 and 75° ($I_{l\theta,45}$) and spectral directional transmittance ($\tau_{\theta,45}$) calculated by:

$$\tau_{n\theta,45} = I_{l\theta,45} / I_{e\theta,45} \qquad (11)$$

These values were then normalised to the zenith value ($\tau_{n\theta,45}$):

$$\tau_{n\theta,45} = \tau_{\theta,45} / \tau_{00} \qquad (12)$$

The zenith transmittance of diffuse light by leaves (τ_{l00}) was measured with the LICOR integrating sphere. The pressed barium sulphate standard was illuminated while a black plug was placed over the measurement port and the spectroradiometer fiber optic tip was mounted in the transmittance port of the sphere (**Plate 2b**).

The radiance of the LICOR sphere measured in this configuration with no leaf in the leaf holder (I_{e00}) and with a leaf present (I_{l00}). Nadir transmittance of diffuse light by a leaf (τ_{l00}) was calculated as:

$$\tau_{l00} = I_{l00} / I_{e00} \qquad (13)$$

The pattern of normalised directional transmittance ($\tau_{l\theta,45}$) measured in the SIS was ascribed to the zenith transmittance τ_{l00} measured by the LICOR instrument to estimate the transmittance $\tau_{l\theta,45}$ at each θ by:

$$\tau_{l\theta,45} = \tau_{n\theta,45}\tau_{l00} \qquad (14)$$

2.6 Estimating Hemispherical Light Flux from Directional Measurements

Each directional measurement of transmitted radiance is only a sample of the total over the hemisphere enclosing the lower surface of the leaf. To completely measure the flux of diffuse light requires many measurements to cover the surface of the hemisphere (**Figure 7**). The number of measurements needed to completely specify the radiance distribution over the hemisphere is impractical. An alternative approach is to sample the radiance in a few directions and to apply a weighting

(a)

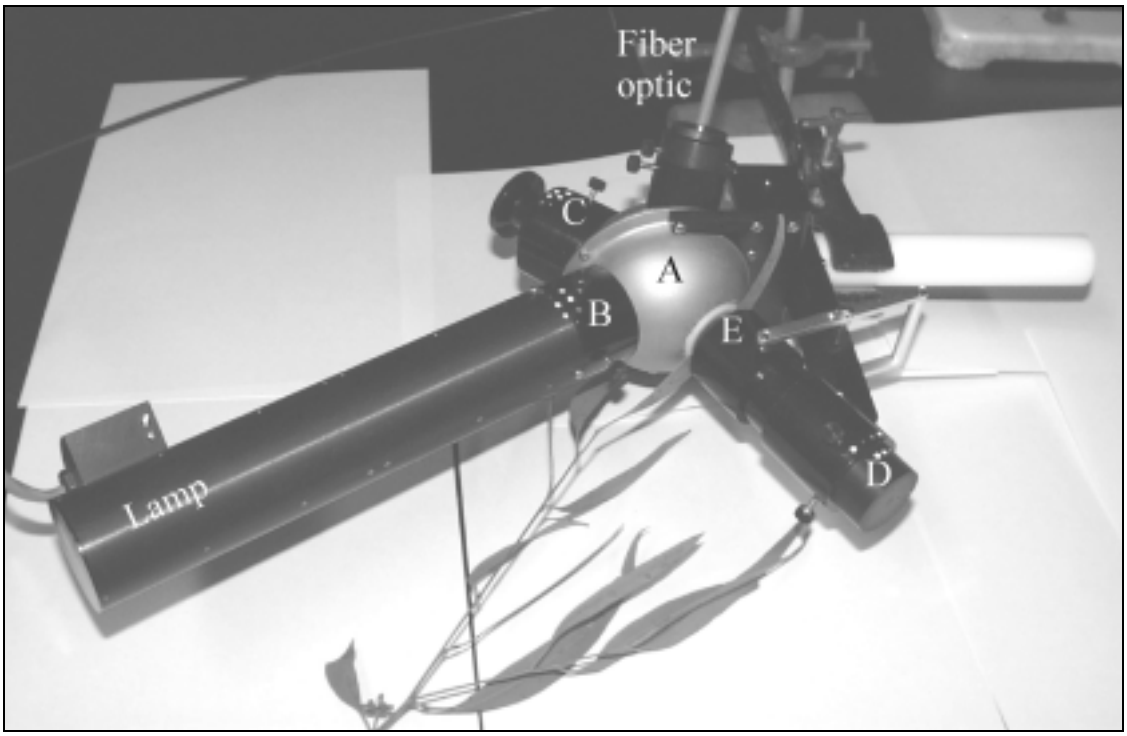

(b)

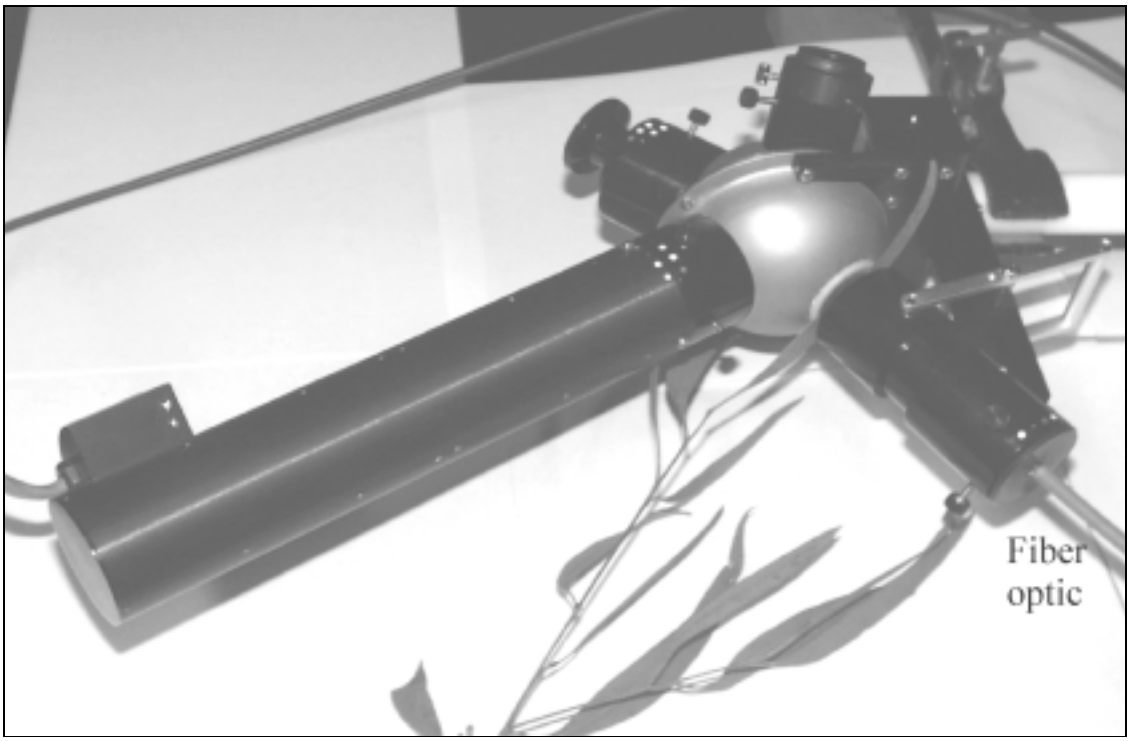

Plate 2. The LICOR 1800-12 integrating sphere configured (a) to measure the hemispherical reflectance of diffuse light. The components of the sphere are; the sphere body (A), the reference lamp port (B), the reflectance lamp port (C), the transmittance lamp port (D) and the sample port (E). The instrument is reconfigured (b) to measure the nadir transmittance of diffuse light by installing the fiber optic in the transmittance port.

factor to account for the proportion of the hemisphere sampled by each measurement (Vogelmann and Björn, 1984). We made six measurements of directional radiance in 15° increments of θ from 0° to 75°, each denoted $\tau_{\theta i}$.

The acceptance angle, usually taken to be the width at half full power, of the measuring device must be known to calculate the weighting factor (Vogelmann and Björn, 1984). By observing a point source of light in a dark enclosure the acceptance angle of the ASD FR spectroradiometer fiber optic tip was estimated as 16°.

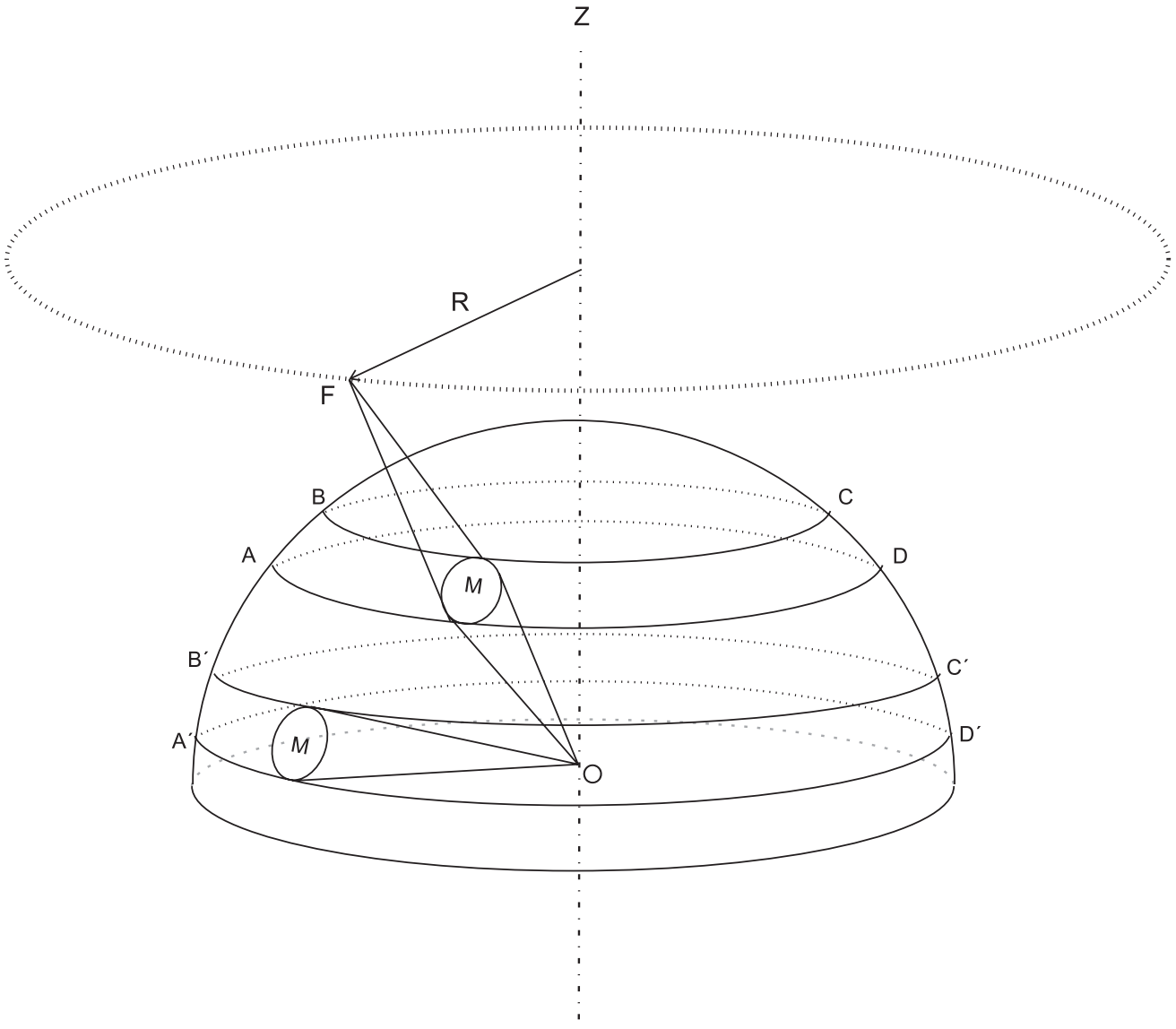

Figure 7. The geometry of measuring an azimuthally constant field of light with a fibre optic. A fibre optic at F with a fixed acceptance angle measures and area M on the surface of an imaginary hemisphere. A light source is located at the center of the hemisphere (O). Moving the fibre around the 'measurement circle', radius R, will keep FO, and hence M, constant while sweeping the measurement spot over the surface of a slice of the hemisphere ABCD. M is kept constant for measurements away from the zenith point (Z) are made by increasing the angle FOZ while keeping the distance FO constant. The area of the hemispherical slice (A´B´C´D´) becomes larger as the angle FOZ is increased. The radius of the measurement circle also becomes larger. However, since FO remains constant, so does the area M therefore more measurements are needed to completely sample the area A´B´C´D´. Estimating the total radiance over the whole hemisphere taking only one measurement at each of six nadir angles (0°,15°,30°,45°,60°,and 75°) requires greater weight on those measurements furthest from the zenith point.

The Vogelmann and Björn (1984) scheme is applied by multiplying the transmittance measurement (τ_θ) at a zenith angle (θ) by the weight appropriate to that zenith angle ($w_{\theta i}$) (**Table 2**). The weighted mean radiance ($\overline{\tau}_h$) over the hemisphere is then calculated by summing the weighted transmittance values and dividing this total by the sum of the weights:

$$\overline{\tau}_h = \frac{\sum_{i=1}^{i=6} \tau_{\theta i} \times w_{\theta i}}{\sum_{i=1}^{i=6} w_{\theta i}} \qquad (15)$$

2.7 Measurements

2.7.1 Measurement procedure

Nine dicotyledonous and seven monocotyledonous leaves were selected for the study. The dicot leaves were selected from growing trees. The monocots were mostly growing in pots. The leaves were selected to encompass as wide a range of leaf thickness as possible within a plant type. For each leaf, we measured the thickness at six locations on the leaf with a spring loaded dial thickness gauge; the mean value was used in subsequent calculations and comparisons. Leaf thickness varied from 278 to 640 μm for the dicots and from 168 to 752 μm for the monocots (**Table 3**).

Dicot leaf thickness was measured while the leaf was attached to the tree. The branch on which the leaf was growing was cut at least 30 cm from the leaf of interest and spectral measurements commenced within one minute with the leaf still attached to the branch. All monocots (except #1) were growing in pots and all spectral and leaf thickness measurements were made with the live leaf still attached to the plant. The leaf of monocot #1 was treated the same as the dicot leaves.

Table 2. The weighting factors of radiance measurements made at six zenith angles in 15° increments between 0° and 75° made with a fiber optic probe of 16° acceptance angle.

Zenith angle	**0°**	**15°**	**30°**	**45°**	**60°**	**75°**
Weight	0.4470	1.3601	2.6275	3.7158	4.5509	5.0759

Table 3. The characteristics of the leaves studied showing the mean thickness of each leaf and the standard deviation (SD) of thickness

Leaf Type	**Species**	**Thickness (μm)**	
		Mean	**SD**
Dicot	*Eucalytpus maniflora*	458	27
	Eucalytpus maniflora	458	12
	Eucalytpus moorii	365	17
	Eucalytpus ceasae	640	21
	Eucalytpus maniflora	387	25
	Eucalytpus maniflori (juvenile)	375	10
	Eucalytpus polyanthemos	337	20
	Eucalytpus dives	278	11
	Eucalyptus pauciflora	*430*	*24*
Monocot	*Angiozanteos flavidius*	575	24
	Ixia maculacata	168	29
	Iris (bare rooted)	323	75
	Iris (potted)	390	32
	Gladiolus.spp	502	27
	Hippiastrum	752	41
	Billbergia nutans	343	5

For each leaf, six separate spectra were measured using various configurations of the LICOR integrating sphere (**Table 4**). The LICOR measurements were made first and were followed immediately by the goniometer measurements (**Table 5**). To test for changes in the leaf's optical properties during the measurement period (typically 10 minutes) the hemispherical reflectance and transmittance of beam light by the leaf was measured again after completing the goniometry. Insignificant changes were found in the leaf spectra over the measurement period.

2.7.2 Calculations

The components of the light balance are calculated as follows (the spectra numbers are those listed in **Tables 4 and 5)**:

1. Hemispherical reflectance of diffuse light ($\rho_{h:h}$); applying **Equation 9** with L_{std} = spectrum 1 and L_{smp} = spectrum 2.
2. Hemispherical transmittance of diffuse light ($\tau_{h:h}$); applying equations 10-12 with spectra 7-13 and equations 12-14 with spectra 4 and 5.
3. Hemispherical reflectance of beam light ($\rho_{h:o}$); spectrum 3/spectrum 2
4. Hemispherical transmittance of beam light ($\tau_{h:o}$); spectrum 6/spectrum 2

Spectra were analysed to find differences between dicot and monocot leaves not between individual leaves. The analyses were carried out both hyperspectrally, using the methods of Price (1994) and in broad wavebands using standard statistical methods (F tests, T tests and analysis of variance).

Table 4. The positioning of the components of the LICOR integrating sphere for measurement of six spectra needed to calculate the light balance of a leaf.

Spectrum		**Lamp Port**			**Sample**	**Instrument**
#	**Description**	**Reference**	**Reflectance**	**Transmittance**	**Port**	**Port**
1	0:h ρ of standard	Lamp	White plug	Black plug	Empty	Fiber optic
2	h:h ρ of leaf	Lamp	White plug	Black plug	Leaf	Fiber optic
3	0:h ρ of leaf	White plug	Lamp	Black plug	Leaf	Fiber optic
4	h:0 τ of leaf	Lamp	White plug	Fiber optic	Leaf	Black plug
5	h:0 τ of standard	Lamp	White plug	Fiber optic	Empty	Black plug
6	0:h τ of leaf	Black plug	White plug	Lamp	Leaf reversed	Fiber optic

See **Plate 2** for the location of the ports referred to in this table

Table 5. The configuration of the satellite illuminating sphere to make six directional measurements of radiance.

Spectrum	7	8	9	10	11	12	13
Zenith angle	0°	0°	15°	30°	45°	60°	75°
Leaf	-	+	+	+	+	+	+

Note: - = leaf absent + = leaf present

3. Results

3.1 Radiometery

All combinations of irradiance and leaf surface exhibit similar radiometric characteristics. **Figure 8** shows a typical set of spectra (Note that the spectra for all leaves are presented in **Appendix A**). Spectral reflectance (ρ) was relatively low in the visible wavelengths (400-700 nm) and due to the expected absorption by photosynthetic pigments, all leaves reflected less blue and red light than they did green. In the red wavelengths (c. 700 nm) ρ increased as the wavelength increased into the near-infrared (NIR). Reflectance then gradually decreased with wavelength until 1300 nm where there was a rapid decline to a trough at the water absorption wavelength near 1400 nm. Beyond 1400 nm ρ increased once more. Spectral transmittance (τ) follows the pattern in ρ with low values in the visible wavelengths, high values in the NIR and declining to trough at about 1400 nm. Absorbance (α), the residual of ρ and τ is high in the visible wavelengths, least in the NIR and peaks again at 1400 nm. (Note: Measurements of ρ under diffuse light show noisy spectra at wavelengths greater than 950 nm owing to the lower signal to noise ratio with this particular instrument configuration).

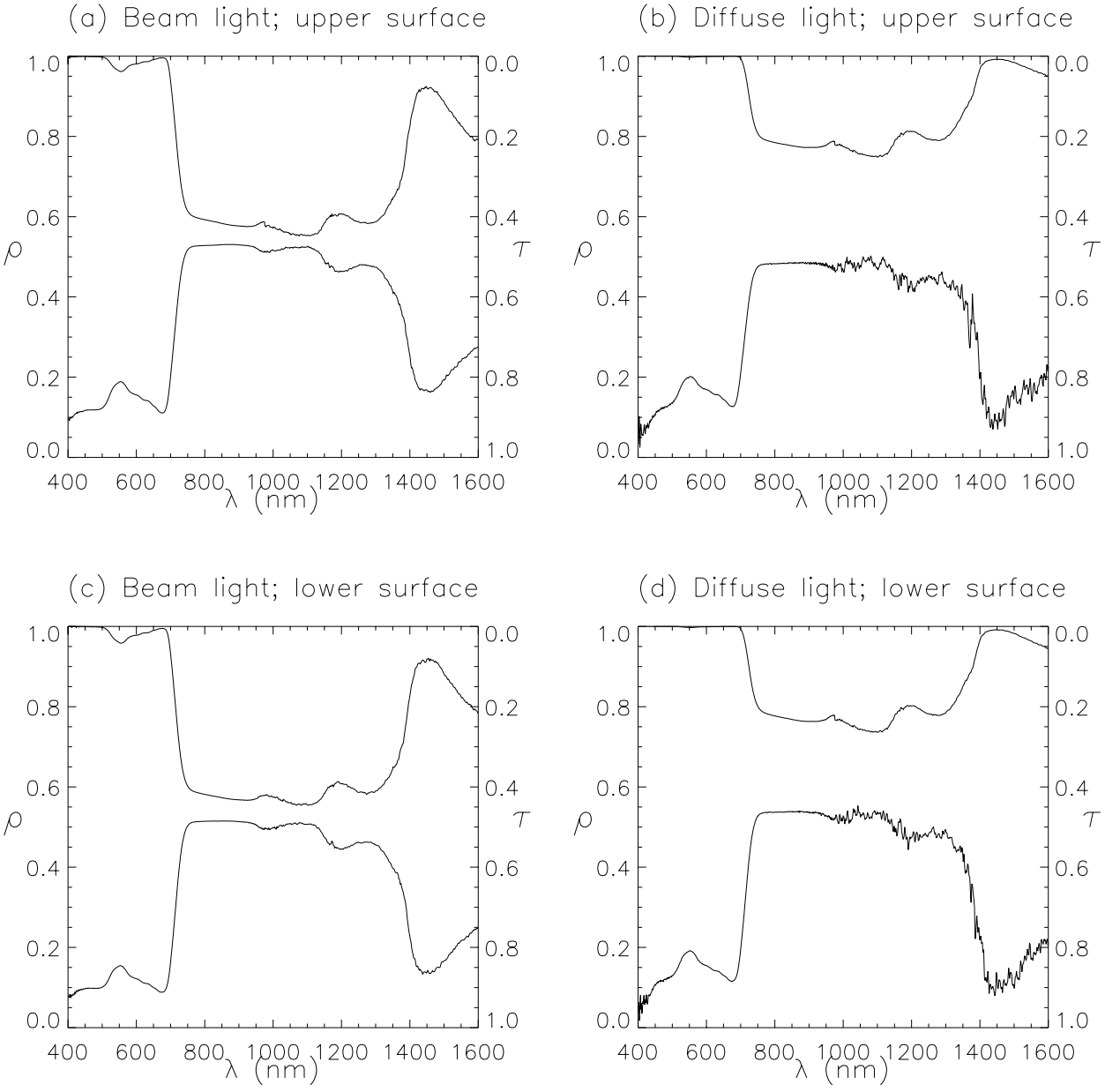

Figure 8. The spectral hemispherical reflectance (ρ) {lower curve} and spectral hemispherical transmittance (τ) {upper curve} of dicot leaf 1 (*E. Moorii*). (a) the upper leaf surface irradiated with beam light, (b) the upper leaf surface irradiated with diffuse light, (c) the lower leaf surface irradiated with beam light and (d) the lower leaf surface irradiated with diffuse light.

Using the root mean square (D) and the angular shape (ω) differences (Price, 1994) between spectra we found that there was more difference within dicot or monocot leaves, than the intrinsic differences between dicot and monocot leaves (**Figure 9, Table 6**).

Given the inability of hyperspectral methods to separate leaf types no further hyperspectral analyses were carried out. Attention was focused on analysing the TM and the AVHRR wavebands. The similarity of the spectral optical properties of upper and lower leaf surfaces was

Table 6. Statistics of the root mean square difference (D) and angular difference (ω) of spectral reflectance. Monocot leaves 1 and 7 were the most different monocot leaf spectra and dicot leaves 3 and 4 the most different dicot leaf spectra.

Source of variation	**D**	ω
Between monocot leaf 1 and monocot leaf 7	0.0595	0.152
Between dicot leaf 3 and dicot leaf 4	0.1293	0.092
Between the mean of dicot and mean of monocot leaves	0.0259	0.046

Note: We use ω in place of θ used by Price (1994)

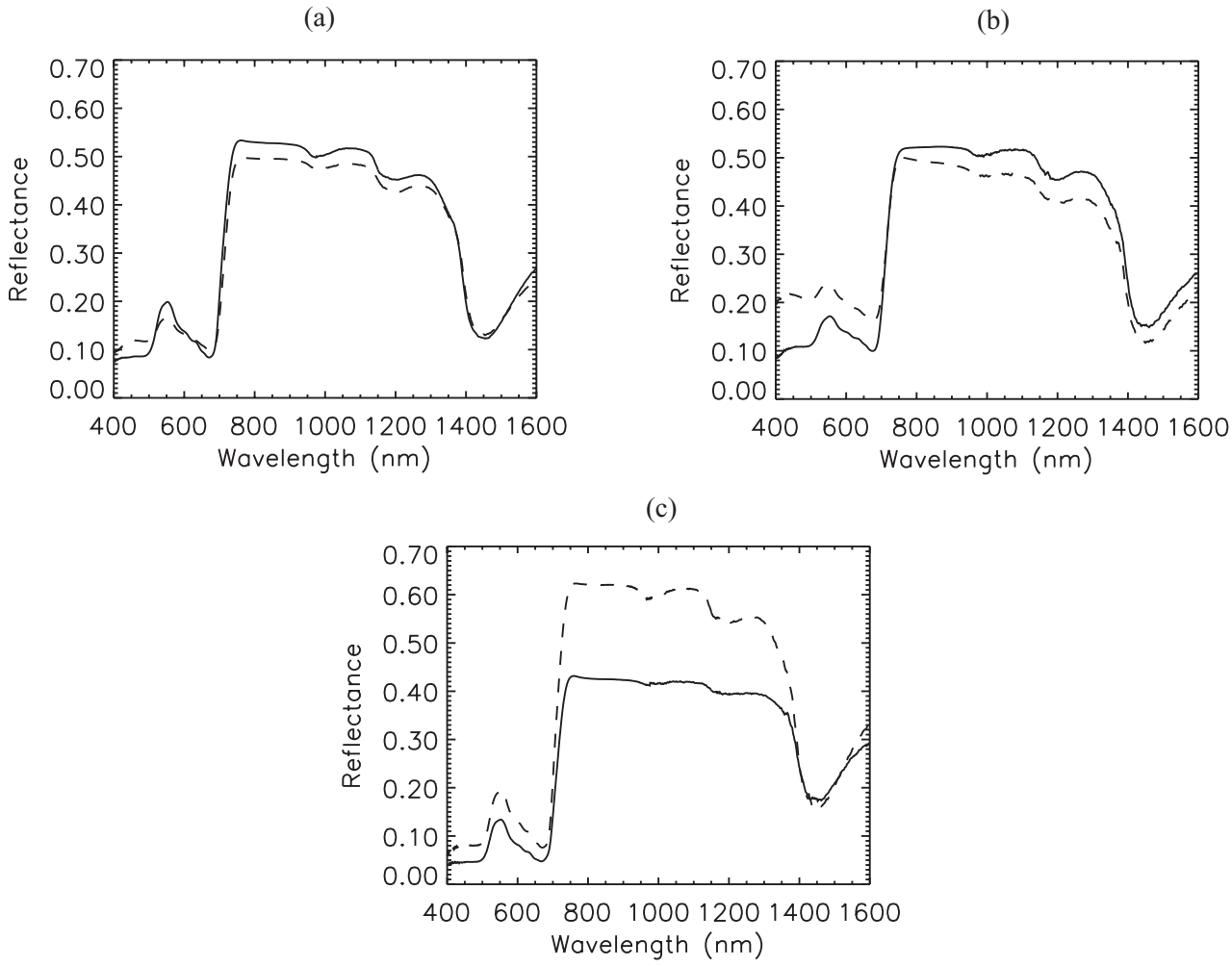

Figure 9. Summary of the spectral reflectance of tree and grass leaves. The mean spectral reflectance of all (a) monocot leaves (n=7, ———) and dicot leaves (n=9, -----); (b) the spectral reflectance of dicot leaf 1 (———) and dicot leaf 7 (-----) and (c) the spectral reflectance of monocot leaf 3 (———) and monocot leaf 4 (----). (Note: leaves with the most different spectra within their class (dicot or monocot) were selected for this analysis)

tested with an F-variance test. This calculated the F statistic and probability that the variance of the spectral reflectance or transmittance of the upper and lower surfaces of a leaf were different. These tests revealed that the optical properties of the upper and lower leaf surfaces were essentially indistinguishable. Of the six wavebands considered, significant differences ($P<0.05$) in reflectance were found only in two wavebands (**Table 7**). The first was the blue TM band (450-520 nm) where the overall reflectance was very low. The second was the NIR wavebands that include the shoulder of rapid change in optical properties. As expected more differences were detected in the narrow TM NIR band (769-900 nm) than in the broader AVHHR NIR band (725-1100 nm).

There was a distinct pattern in the directional transmittance (τ) of diffuse irradiance in red and NIR wavelengths. Directional τ relative to that at zenith (τ_{rel}) was highest normal to the leaf surface and decreased with θ to very low values at large θ (**Figures 10a and b**). The τ_{rel} of red wavelengths was higher than that of NIR for both dicot and monocot leaves at all θ (**Figures 10c and d**). τ_{rel} of both red and NIR by monocot leaves was lower than that of dicot leaves where θ was less than 60° (**Figures 10a and b**). At θ greater than 60° τ_{rel} by moncot leaves was less than that of dicot leaves (**Figure 10a and b**). Analysis of variance showed that at zenith angles of 60° and 75° τ_{rel} of red light by dicot and monocot leaves was similar and that all other comparisons of τ_{rel} at a given zenith angle were different ($P<0.05$) (**Table 8**). τ_{rel} decreased with θ, the decrease was more marked in the red wavelengths. The dependence of τ_{rel} on θ for both red and NIR light is well described by second order polynomials (**Table 8**).

The consequence of illuminating either the top or bottom surface of a leaf on its optical properties was investigated in TM and AVHRR bandwidths. We did this by calculating the Student's T-statistic, and the probability, that the mean ρ or τ of the leaf's top surface was different from that of its bottom surface. We found that the average optical properties of the top and bottom surfaces of leaves were similar ($P<0.05$) in all measured bandwidths (Tables of these summary statistics are presented in **Appendix B**).

Table 7. The number of F-variance tests that found significant differences between the hemispherical reflectance and transmittance of the upper and lower leaf surfaces. The values in the body of the table are the number of significant tests found for dicot leaves + monocot leaves = Total.

Waveband		**Beam irradiance**		**Diffuse irradiance**	
(nm)	**Satellite equivalent**	ρ	τ	ρ	τ
450-520	TM 1	4 + 0 = 4	0 + 0 = 0	0 + 0 = 0	0 + 1 =0
520-600	TM 2	1 + 1 = 2	0 + 0 = 0	1 + 0 = 0	0 + 0 = 0
630-690	TM 3	1 + 0 = 1	0 + 0 = 0	0 + 0 = 0	0 + 1 = 1
769-900	TM 4	5 + 5 = 10	0 + 1 =1	6 + 4 = 10	0 + 2 = 2
580-680	AVHRR 1	0 + 0 = 0	0 + 0 = 0	0 + 0 = 0	0 + 1 = 1
725-1100	AVHRR 2	0 + 1 = 1	2 + 1 = 3	3 + 2 =5	1 + 3 = 5

(Note: 17 tests are carried out in each waveband)

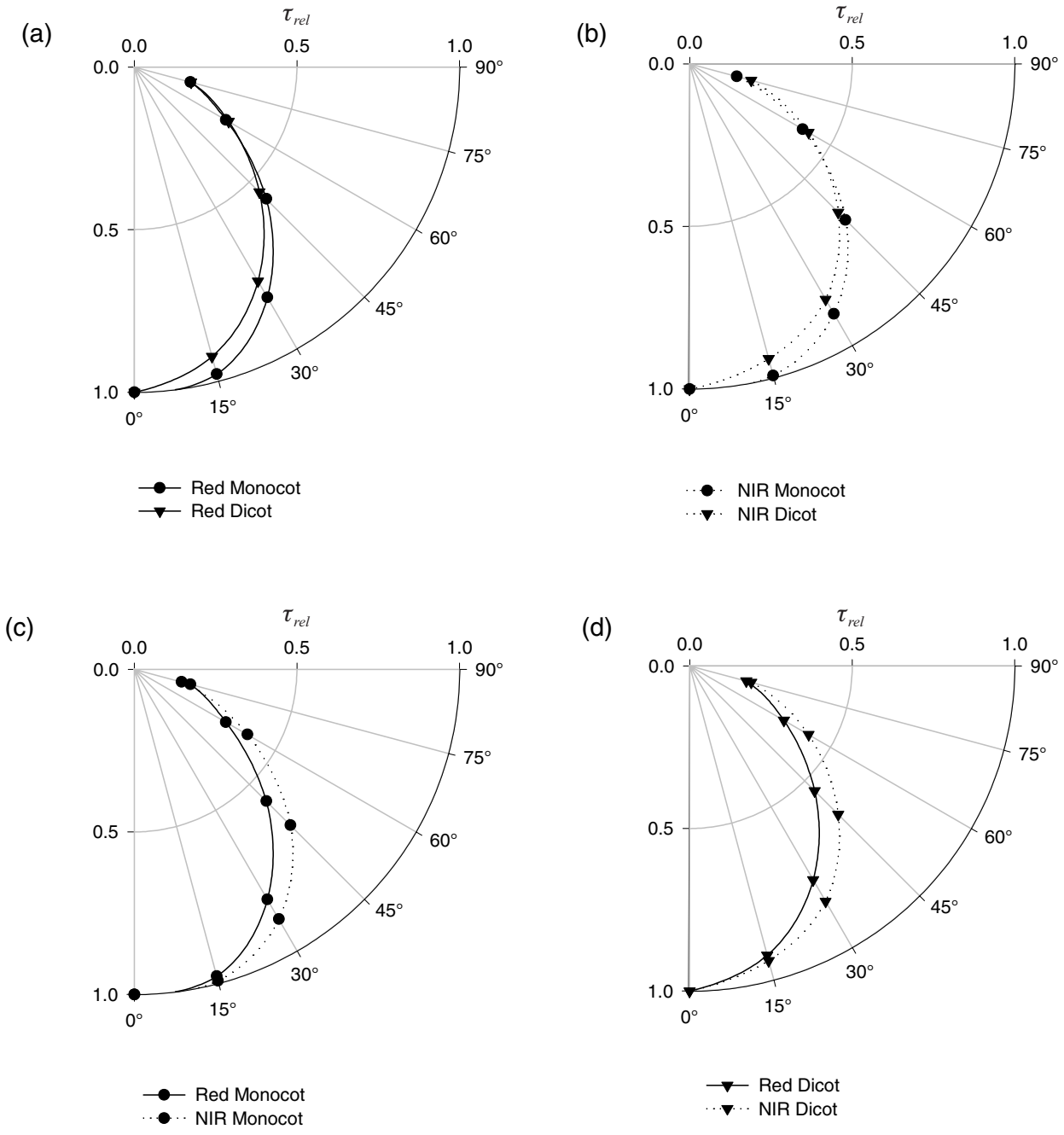

Figure 10. The average directional transmittance (τ_{rel}) of diffuse red (λ 580 - 680 nm) (———) and NIR (λ 725 - 100 nm) (·····) light by monocot (●) and dicot (▼) leaves. Comparing τ_{rel} of (a) red light by dicots and monocots; (b) NIR light by dicots and monocots; (c) red and NIR light by monocots and (d) red and NIR light by dicots.

3.2 Leaf Light Balance

The leaf light balance analysis was carried out in two AVHRR broad wavebands; red (580-680 nm) and near-infrared (725-1100 nm), denoted R and NIR. There were minimal effects in the red waveband of changing from illumination with beam to diffuse light (**Figure 11a**); the average reflectance of leaves increased slightly (ρ_{rb} = 0.109, ρ_{rd} = 0.136). Transmittance of red light decreased (τ_{rb} = 0.026, τ_{rd} = 0.002). Despite the large relative decrease in transmittance, the net effect was virtually no change in the absorbance of red light since τ is such a small component of the light balance at these wavelengths. The mean absorbencies were α_{rb} = 0.87 and α_{rd} = 0.86.

Table 8. The mean directional transmittance of diffuse light by leaves relative to the transmittance of diffuse light at nadir. Transmittance of red (λ 580 - 680 nm) and NIR (λ 725 - 1100 nm) was measured at five zenith angles.

Leaf Type (N)	**Wavelength**	**Zenith angle**				
		15°	**30°**	**45°**	**60°**	**75°**
Dicot (7)	NIR	0.9916	0.8873	0.6779	0.4011	0.1501
	Red	0.9771	0.8173	0.5729	0.3245a	0.1779b
Monocot (9)	NIR	0.9387	0.8362	0.6464	0.4223	0.1959
	Red	0.9212	0.7599	0.5437	0.3344a	0.1803b

Note: When comparing within the columns of **Table 8** values marked with the same letters are statistically similar (P<0.05). All other comparisons within columns are statistically different (P<0.05). θ and the τ_{rel} are related by second order polynomials:

$$\tau_{relred} = 0.9231\theta^2 - 0.0421\theta + 0.1258 \qquad r^2 = 0.9949$$
$$\tau_{relNIR} = 0.1324\theta^2 + 0.9679\theta - 0.0916 \qquad r^2 = 0.9949$$

where: τ_{relRed} = the directional transmittance in the red wavelengths
τ_{relNIR} = the directional transmittance in the NIR wavelengths

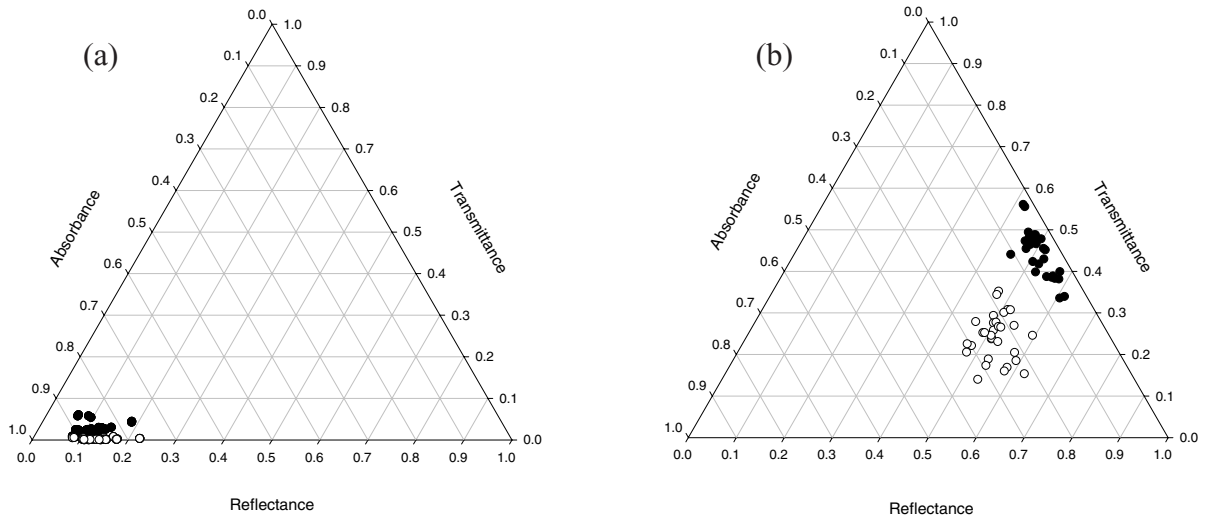

Figure 11. Ternary diagram showing the optical properties of each leaf (a) red (λ 580-680 nm) and (b) NIR (λ 725-1100 nm) parts of the spectrum. Measurements made while irradiating the top and bottom leaf surface of each leaf are presented. Illumination was with either beam (●) or diffuse (O) light.

The near-infrared light balance was much more affected by changing from irradiance with beam to diffuse light (**Figure 11b**). The mean reflectances were similar (ρ_{nirb} = 0.50, ρ_{nird} = 0.52) (P<0.05). The mean ρ_{nird} of dicot leaves (0.490) was slightly lower than the mean ρ_{nirb} of monocot leaves (0.518), but it would be difficult to distinguish between these groups of leaves by their reflectance (**Figure 12**). However, the mean τ_{nird} of all leaves (0.25) was almost half that of τ_{nirb} (0.45). The consequence of this reduced transmittance of near-infrared light was a substantial increase in absorbance from α_{nirb} = 0.05 to α_{nird} = 0.24.

We found that variation in the components of the NIR light balance (**Figure 11b**) was related to leaf thickness (z). In general, there is a slight increase in reflectance with z and that the trends in ρ_{nirb} and ρ_{nird} with z were similar (**Figure 13a**). Transmittance declined with leaf thickness (**Figure 13b**) and there was a clear separation of τ_{nirb} and τ_{nird}, although the slopes of the relationships between z and τ_{nirb} and z and τ_{nird} similar. The decrease in z and transmittance with z results in a corresponding increase in absorbance. As with τ, there was a clear separation of the relationships between z and α_{nirb} and z and α_{nird} (**Figure 13c**). Both the slope and the intercept of the relationship between z and α_{nird} were statistically significant (P < 0.05), while there was no significant relationship between z and α_{nirb}. In no instance did we find separate relationships between z and ρ, z and τ or z and α for dictot and monocot leaves.

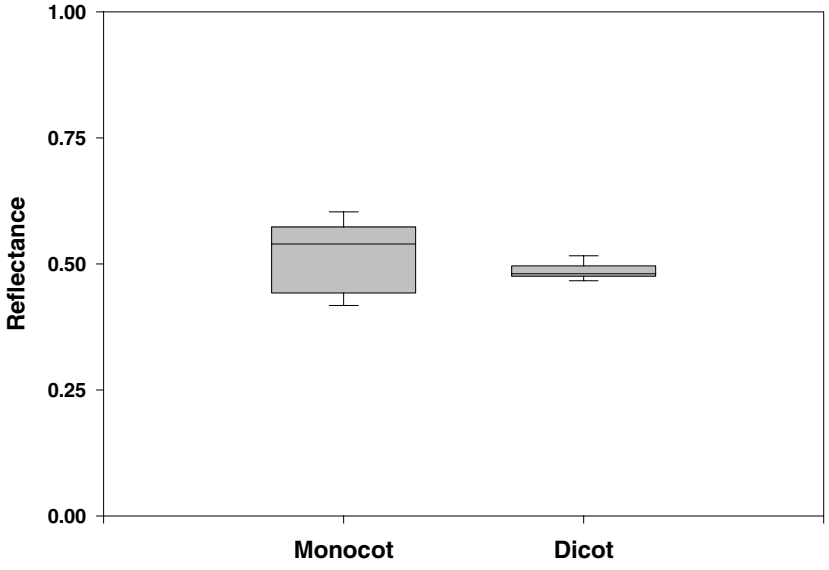

Figure 12. Summary of the reflectance of beam near-infrared (λ 725 - 1100 nm) light by dicot and monocot leaves. The top and bottom of the box denote the 25th and 75th centiles, the central line is the median, and the outer bars are the 10th and 90th centiles of reflectance.

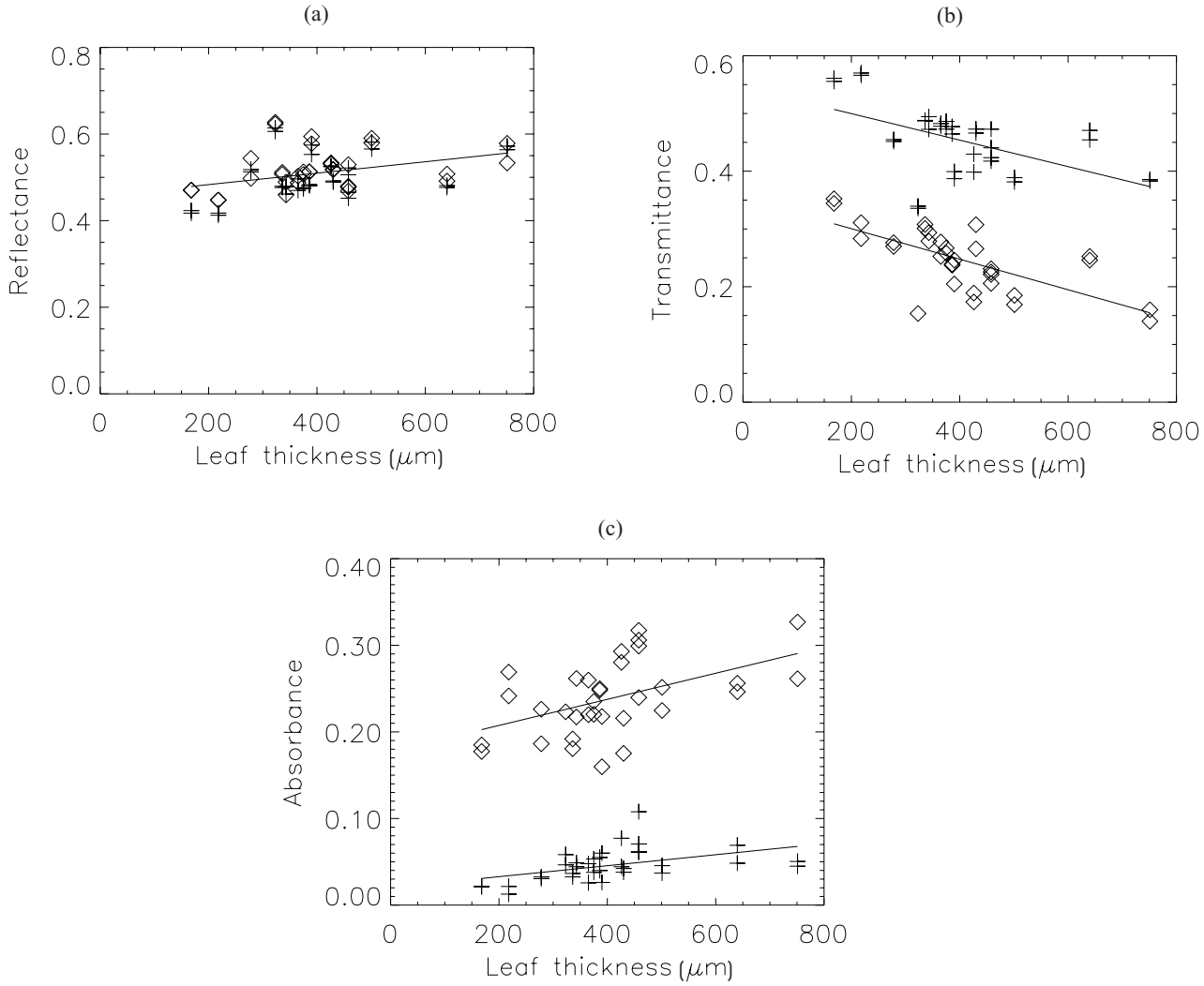

Figure 13. The (a) reflectance (b) transmittance and (c) absorbance in the near-infrared (725-1100 nm) of beam (+) and diffuse (◇) radiance as a function of leaf thickness.

4. Discussion

We found that the transmission of diffuse light through leaves was not isotropic. Light incident at oblique angles is more likely to be absorbed than light incident moving normal or near normal to the surface. If the leaf was considered as a uniform optically thick medium, then light passing through the leaf would be attenuated in proportion to its path length through the leaf, and transmittance would be proportional to $\cos\theta$. We found that transmittance was lower than could be explained path length through the leaf. This finding suggests that the internal structure of leaves is such that more light is transmitted at angles close to the leaf normal. Since this anisotropy of transmittance was marginally greater in dicot leaves it is consistent with the proposition of Smith et al. (1997), who suggested that dicot leaves evolved to focus light within the leaf to optimise gradients of light and CO_2.

We observed that leaf reflectance was relatively constant, but thicker leaves tended to have slightly lower transmittance and hence higher absorbance. However, there was a lot of scatter in these relationships (**Figure 13**). We expected this, because the volume fraction of air space tends to be low in thin leaves, but can be either high or low in thick leaves (Roderick et al., 1999). Thus a thick leaf, with a large volume fraction of internal spaces, would likely transmit much more light than a leaf of the same thickness with fewer internal air spaces. For example, Stalon et al. (2001) found that the NIR reflectance of the leaves of 48 species was unrelated to their thickness, a result that suggests that inter-species variability in leaf optical properties dominates any generic relationship with leaf thickness. Baldini et al. (1997) found that variations in leaf optical properties induced by changes in leaf water content were larger than changes with leaf thickness. Since NIR reflectance and leaf thickness are not related in a regular way, we cannot use reflectance to predict the thickness and the associated function of leaves.

Our measurements showed that there were no consistent differences in the optical properties of dicot and monocot leaves. This is an important finding because it means that monocot and docot leaves cannot be distinguished by their spectral reflectance, in either specific narrow wavelength intervals or over broader bands typical of satellite instruments. Despite that, it is well known that the bulk reflectance of forests, as observed in satellite images, is in general much lower than the reflectance from grasslands/croplands, particularly in the near-infrared. If this difference is not due to the leaves themselves, then it can only be caused by more shade within tree canopies than within grass canopies, as implied by the results of Hall et al. (1995).

In visible wavelengths we found that leaves absorbed roughly the same proportions of diffuse and beam light. It is well known (see for example Choudhury, 2000, Hammer and Wright, 1994, Healey et al., 1998) that plant canopies use diffuse visible light more efficiently in photosynthesis than they do beam. Thus, because there were no differences in the optical properties of the leaves in the visible, this efficiency gain must be for some other reason, such as less shadow within the plant canopy under diffuse radiance (Roderick et al., 2001).

The high absorbance of diffuse near-infrared light was our most striking finding. About 24% of diffuse light was absorbed compared with only 5% of beam light. This was a surprise, because as far as we know it has not previously been reported. Walter-Shea et al. (1989) observed that the absorption of beam NIR light by leaves increased markedly as the incidence angle increased. Diffuse light has components coming from all directions; the absorbance of those components incident at high angles would be higher, implying absorption of diffuse near-infrared light would be much higher than of beam. This is exactly what we observed. The same principles should hold for light of visible wavelengths. However, the effect would not be as large in the visible, because almost all visible light is absorbed by plant pigments, irrespective of the illumination direction. Walter-Shea et al. (1989) also showed that the transmittance of visible light was relatively independent of the direction from which the leaf was irradiated. That is consistent with our observations in visible wavelengths, where we measured almost no differences in the optical properties of leaves irradiated with either beam or diffuse.

Existing canopy energy balance models (for example Wang and Leuning, 1998, De Pury and Farquhar, 1997) generally assume that the optical properties of leaves are constant. Our results suggest that these models would significantly underestimate the NIR absorbed on cloudy days when diffuse radiation dominates. This will, in turn, give rise to errors in model estimates of leaf temperature, rates of transpiration and other temperature dependant leaf scale processes.

5. Conclusions

This research found that:

1. The transmittance of diffuse light by dicot and monocot leaves was anisotropic. But this does not affect the bulk optical properties of dicot and monocot leaves.
2. Dicot and monocot leaves could not be distinguished by either hyperspectral or broadband analysis of their reflectance.
3. As leaf thickness increased, the spectral reflectance and spectral absorbance factors increased slightly, while the spectral transmittance factor decreased, but we did not make enough measurements to establish whether these trends are general. The absorption of diffuse near-infrared radiance (about 24%) is much higher than of beam (about 5%) irradiance. These differences need to be accounted for when modelling the energy balance of vegetation canopies.

6. References

ASD (1999), FieldSpec users guide. Analytical Spectral Devices, Inc, Boulder, Colorado.

Asner, G.P. (1998), Biophysical and biochemical sources of variability in canopy reflectance. Remote Sensing of Environment, 64:234-253.

Baldini, E., Facini, O., Nerozzi, F., Rossi, F. and Rotondi, A. (1997), Leaf characteristics and optical properties of different woody species. Tree, 12:73-81.

Brondizio, E., Moran, E., Mausel, P. and Wu, Y. (1996), Land cover in the Amazon estury: linking of the Thematic Mapper with botanical and historical data. Photogrammetric Engineering and Remote Sensing, 62:921-926.

Choudhury, B.L. (2000), A sensitive analysis of the radiation use efficiency for gross photosynthesis and net carbon accumulation by wheat. Agricultural and Forest Meteorology, 101:217-234.

Cracknell, A.P. (1997), The Advanced Very High Resolution Radiometer, Taylor and Francis, London.

De Pury, D.E. and Farquhar, G.D. (1997), Simple scaling of photosynthesis from leaves to canopies without the errors of big-leaf models. Plant, Cell and Environment, 20:537-557.

Fiorella, M. and Ripple, W.J. (1993), Determining successional stage of temperate coniferous forests with Landsat satellite data. Photogrammetric Engineering and Remote Sensing, 59:239-246.

Hall, F.G., Shimabukuro, Y.E. and Huemmrich, K.F. (1995), Remote sensing of forest biophysical structure using mixture decomposition and geometric reflectance models. Ecological Applications, 5:993-1013.

Hammer, G.L. and Wright, G.C. (1994), A theoretical analysis of nitrogen and radiation effects on radiation use efficiency in peanut. Australian Journal of Agricultural Research, 45:575-589.

Healey, K.D., Rickert, K.G., Hammer, G.L. and Bange, M.P. (1998), Radiation use efficiency increases when the diffuse component of incident radiation is enhanced under shade. Australian Journal of Agricultural Research, 49:665-672.

Knapp, A.K. and Carter, G.A. (1998), Variability in leaf optical properties among 26 species from a broad range of habitats. American Journal of Botany, 87:940-946.

Labsphere (1997), Diffuse reflectance coatings and materials, Catalog 1. Labsphere, Inc., North Sutton, New Hampshire.

Labsphere (1999), A guide to integrating sphere theory and applications. Tech Guide, Labsphere, Inc., North Sutton, New Hampshire.

LI-COR (1984), LI_1800UW Underwater spectroradiometer instruction manual. Publication no. 8405-0037 LI-COR Inc, Linclon, Nabraska.

Matherson, W. and Ringrose, S. (1994), The development of image processing techniques to assess changes in green vegetation cover along a climatic gradient through Northern Territory, Australia. International Journal of Remote Sensing, 15:17-47.

McCloy, K. and Hall, K.A. (1991), Mapping the density of woody vegetation cover using Landsat MSS digital data. International Journal of Remote Sensing, 12:1877-1886.

Price, J.C. (1994), How unique are spectral signatures. Remote Sensing of Environment, 48:181-186.

Roderick, M.L., Berry, S.L., Nobel, I.R. and Farquhar, G.D. (1999), A theoretical approach to linking the composition and morphology with function of leaves. Functional Ecology, 13:683-695.

Roderick, M.L., Farquhar, G.D., Berry, S.L. and Nobel, I.R. (2001), On the direct effect of clouds and atmospheric particles on productivity and structure of vegetation. Oecoliga, 129:21-30.

Smith, W.K., Vogelmann, T.C., DeLucia, E.H., Bell, D.T. and Shepherd, K.A. (1997), Leaf form and photosynthesis. BioScience, 47:785-793.

Stalon, M.R., Hunt, R.E.J. and Smith, W.K. (2001), Estimating near-infrared leaf reflectance from leaf structural characteristics. American Journal of Botany, 88:278-284.

Steininger, M.K. (1996), Tropical secondary forest regrowth in the Amazon: age, area and change estimation with Thematic Mapper data. International Journal of Remote Sensing, 17:9-27.

Vogelmann, T.C. and Martin, G. (1993), The functional significance of pallisade tissue: penetration of directional versus diffuse light. Plant, Cell and Environment, 16:65-72.

Vogelmann, T.C. and Björn, L.O. (1984), Measurement of light gradients and spectral regime in plant tissue with a fibre optic probe. Physiolgia Plantarum, 60:361-368.

Walter-Shea, E.A., Norman, J.M. and Blad, B.L. (1989), Leaf bidirectional reflectance and transmittance in corn and soybean. Remote Sensing of Environment, 29:161-174.

Wang, Y.P. and Leuning, R. (1998), A two-leaf model for canopy conductance, photsysnthesis and partitioning of available energy I: Model description and comparison with a multi-layered model. Agricultural and Forest Meteorology, 91:89-111.

Appendix A

This appendix contains figures of the spectral hemispherical reflectance and hemispherical transmittance of all leaves in the experiment. A table of the results of the F-variance test of difference between the top and bottom surfaces of each leaf is given with each figure. The F-variance tests were conducted over specific wavebands in the visible and near-infrared wavelengths. These wavebands correspond with those of the Landsat Thematic Mapper and National Oceanic and of the Atmospheric Administration Advanced Very High Resolution Radiometer.

Figure A1. The spectral hemispherical reflectance (ρ) {lower curve} and spectral hemispherical transmittance(τ) {upper curve} of dicot leaf 1 (*Eucalyptus maniflora*). (a) The upper leaf surface irradiated with beam light, (b) the upper leaf surface irradiated with diffuse light, (c) the lower leaf surface irradiated with beam light and (d) the lower leaf surface irradiated with diffuse light.

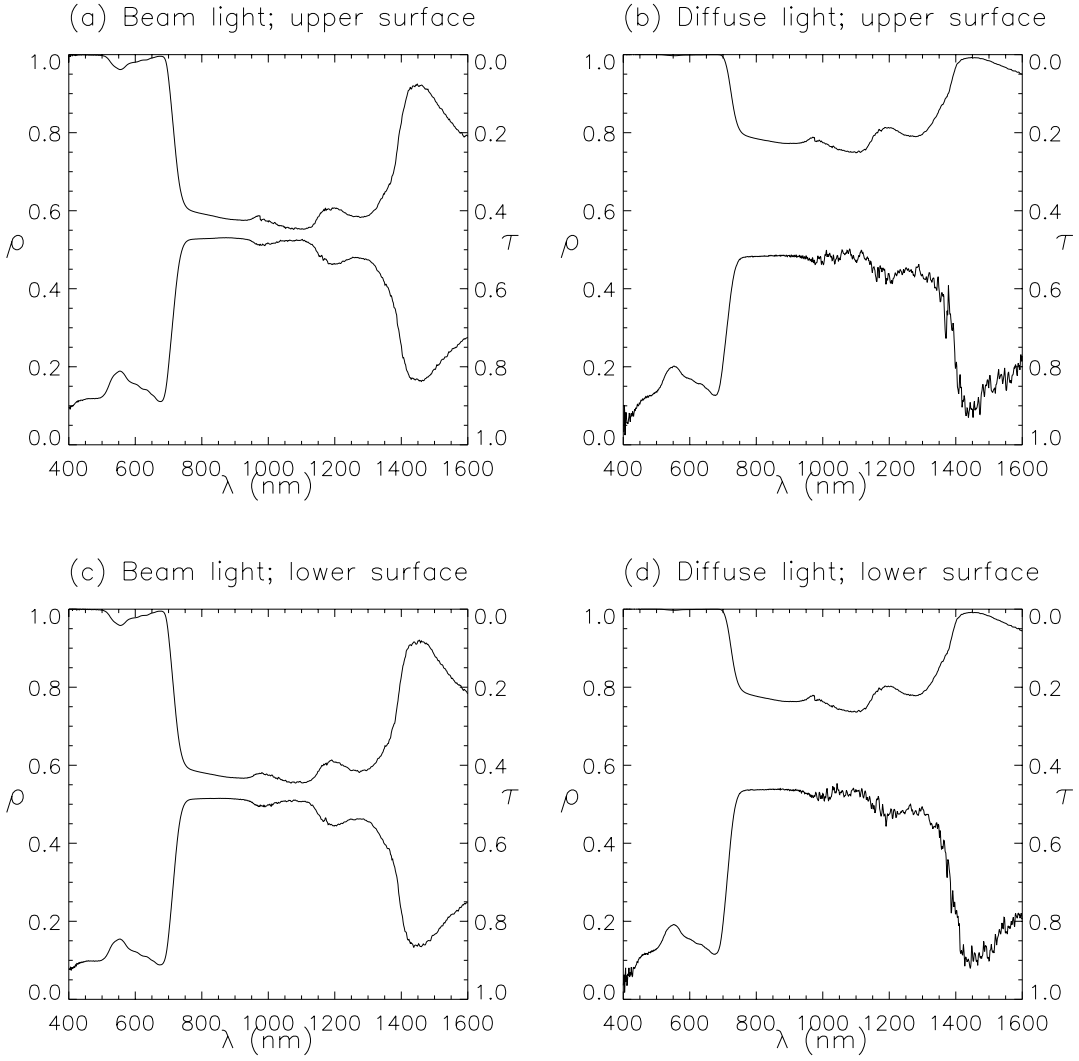

Table A1. Comparing the top and bottom surfaces of dicot leaf 1 (*Eucalyptus maniflora*). The F-variance statistic (F) and the probability (P) that the spectra of the top and bottom surfaces have significantly different variances are shown.

Band (Wavelength)	Beam Light				Diffuse Light			
	ρ		τ		ρ		τ	
	F	P	F	P	F	P	F	P
TM1 (450-520)	1.9303	0.0070	1.3199	0.2515	1.3215	0.2494	******	******
TM2 (520- 600)	1.1029	0.6643	1.1314	0.5844	1.2224	0.3741	1.0648	0.7810
TM3 (630- 690)	2.0667	0.0060	1.2953	0.3231	1.4039	0.1955	1.0269	0.9192
TM4 (769- 900)	4.4156	0.0000	1.2614	0.1870	2.0092	0.0001	1.1845	0.3355
AVHRR1 (580- 680)	1.6575	0.0126	1.2134	0.3374	1.1245	0.5605	1.0481	0.8156
AVHRR2 (725-1100)	1.1960	0.0839	1.3468	0.0041	1.4761	0.0002	1.1867	0.0984

Note: ****** denotes missing data

Figure A2. The spectral hemispherical reflectance (ρ) {lower curve} and spectral hemispherical transmittance(τ) {upper curve} of dicot leaf 2 (*Eucalyptus maniflora*). (a) The upper leaf surface irradiated with beam light, (b) the upper leaf surface irradiated with diffuse light, (c) the lower leaf surface irradiated with beam light and (d) the lower leaf surface irradiated with diffuse light.

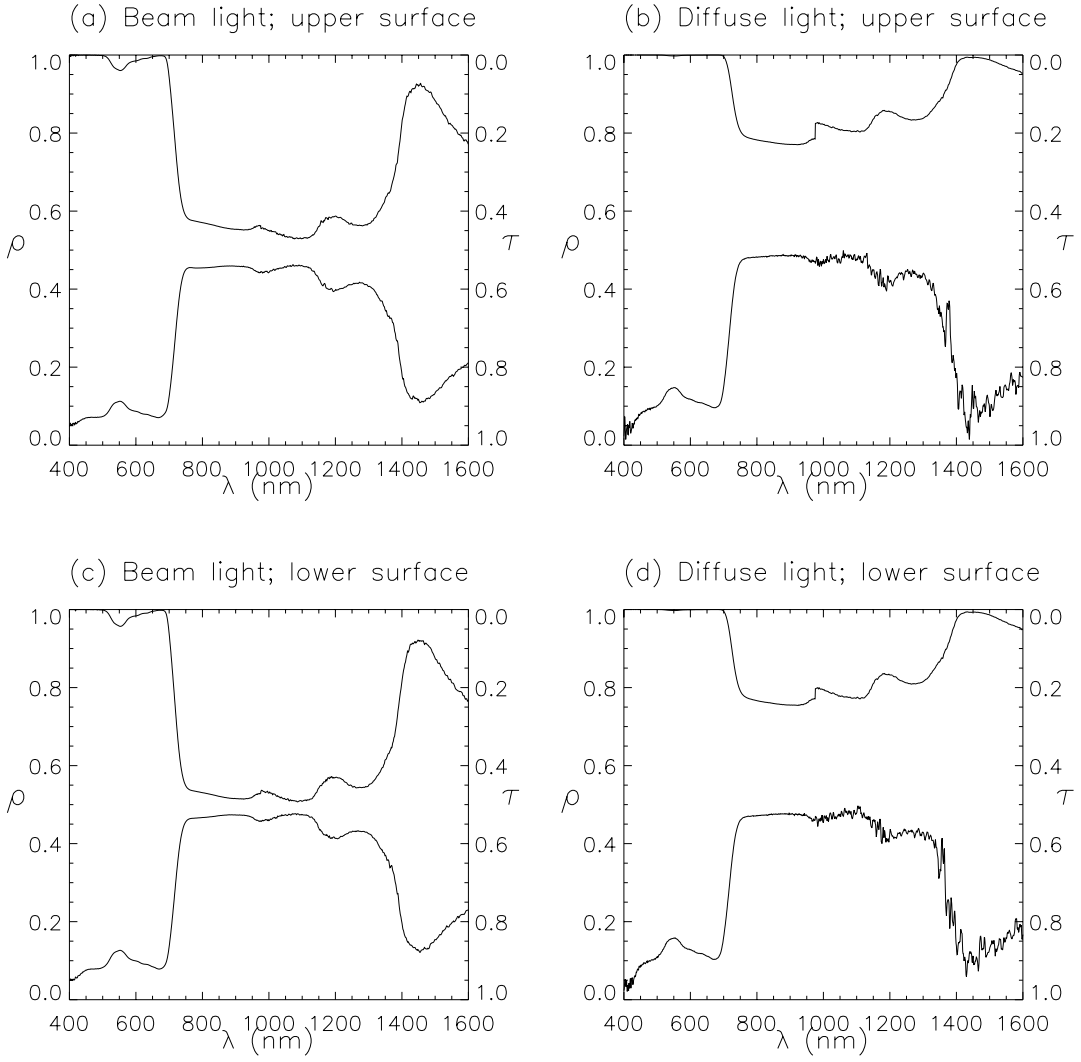

Table A2. Comparing the top and bottom surfaces of dicot leaf 2 (*Eucalyptus maniflora*). The F-variance statistic (F) and the probability (P) that the spectra of the top and bottom surfaces have significantly different variances are shown.

Band (Wavelength)	Beam Light				Diffuse Light			
	ρ		τ		ρ		τ	
	F	P	F	P	F	P	F	P
TM1 (450-520)	1.7406	0.0227	1.1856	0.4813	1.3582	0.2061	******	******
TM2 (520- 600)	1.1064	0.6542	1.1800	0.4636	1.0191	0.9333	1.0865	0.7133
TM3 (630- 690)	1.4403	0.1641	1.1664	0.5562	1.4830	0.1330	1.1083	0.6943
TM4 (769- 900)	2.3303	0.0000	1.1950	0.3112	1.2317	0.2362	1.0200	0.9103
AVHRR1 (580- 680)	1.5541	0.0293	1.1827	0.4054	1.2673	0.2403	1.1011	0.6328
AVHRR2 (725-1100)	1.1892	0.0943	1.2189	0.0560	1.1121	0.3049	1.1561	0.1611

Note: ****** denotes missing data

Figure A3. The spectral hemispherical reflectance (ρ) {lower curve} and spectral hemispherical transmittance(τ) {upper curve} of dicot leaf 3 (*Eucalyptus moorii*). (a) The upper leaf surface irradiated with beam light, (b) the upper leaf surface irradiated with diffuse light, (c) the lower leaf surface irradiated with beam light and (d) the lower leaf surface irradiated with diffuse light.

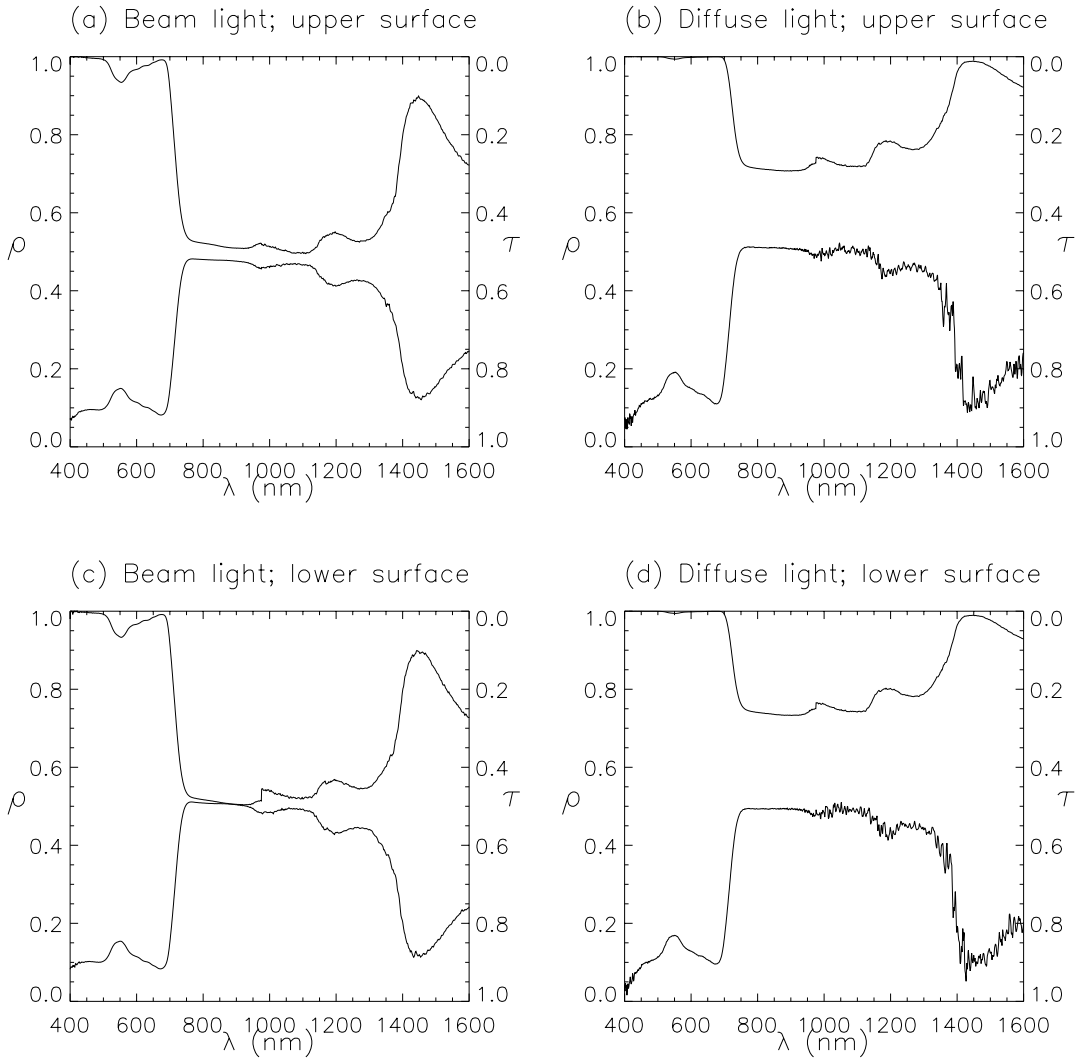

Table A3. Comparing the top and bottom surfaces of dicot leaf 3 (*Eucalyptus moorii*). The F-variance statistic (F) and the probability (P) that the spectra of the top and bottom surfaces have significantly different variances are shown.

Band (Wavelength)	Beam Light				Diffuse Light			
	ρ		τ		ρ		τ	
	F	P	F	P	F	P	F	P
TM1 (450-520)	1.0334	0.8920	1.0597	0.8103	1.0604	0.8082	1.2847	0.3005
TM2 (520- 600)	1.2326	0.3547	1.0344	0.8808	1.0160	0.9440	1.2240	0.3710
TM3 (630- 690)	1.2442	0.4038	1.0189	0.9430	1.6497	0.0568	1.3049	0.3095
TM4 (769- 900)	1.2007	0.2984	1.1756	0.3577	3.6858	0.0000	1.2367	0.2273
AVHRR1 (580- 680)	1.0082	0.9676	1.0160	0.9372	1.3428	0.1442	1.2664	0.2418
AVHRR2 (725-1100)	1.2011	0.0768	1.1324	0.2299	1.0432	0.6829	1.1664	0.1372

Figure A4. The spectral hemispherical reflectance (ρ) {lower curve} and spectral hemispherical transmittance(τ) {upper curve} of dicot leaf 4 (*Eucalyptus ceasae*). (a) The upper leaf surface irradiated with beam light, (b) the upper leaf surface irradiated with diffuse light, (c) the lower leaf surface irradiated with beam light and (d) the lower leaf surface irradiated with diffuse light.

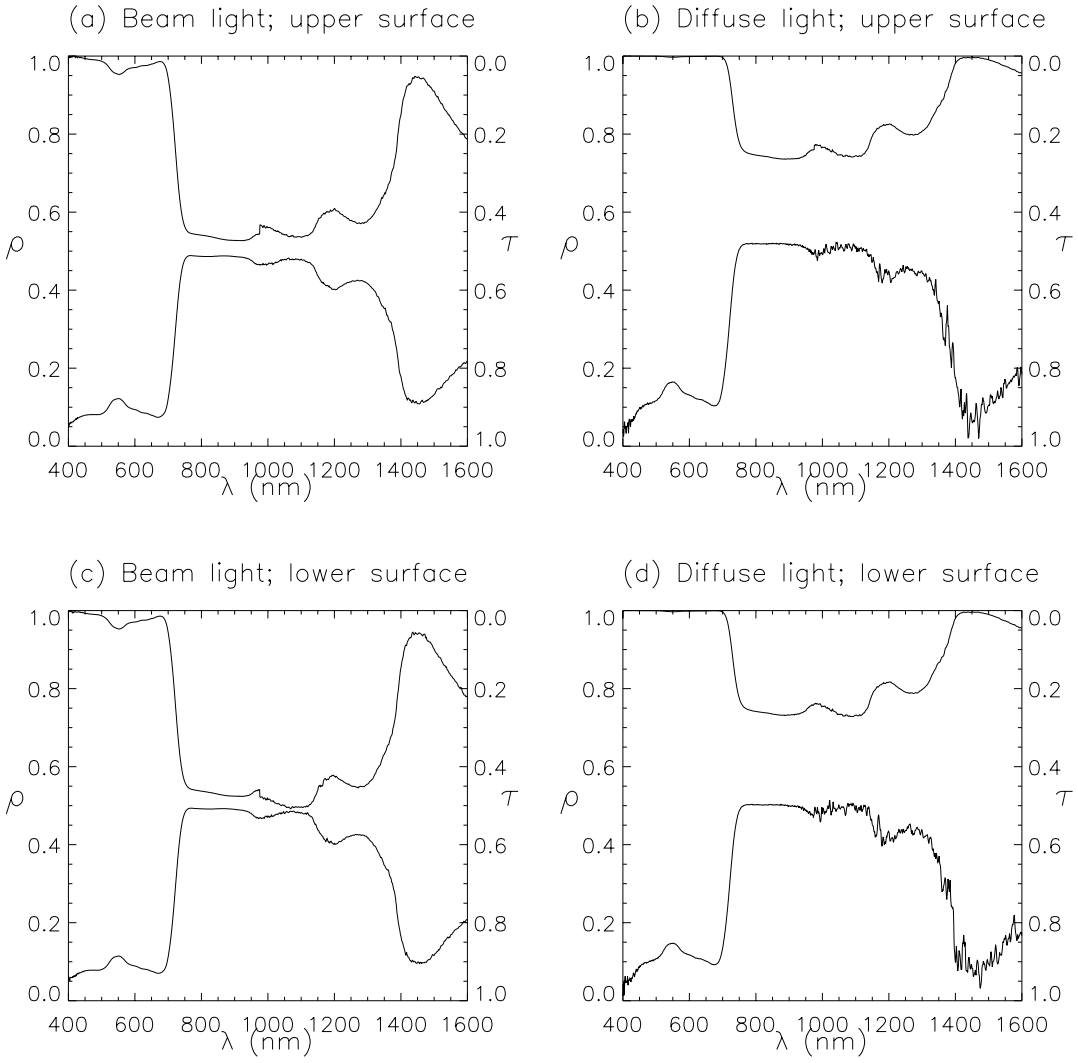

Table A4. Comparing the top and bottom surfaces of dicot leaf 4 (*Eucalyptus ceasae*). The F-variance statistic (F) and the probability (P) that the spectra of the top and bottom surfaces have significantly different variances are shown.

Band (Wavelength)	Beam Light				Diffuse Light			
	ρ		τ		ρ		τ	
	F	P	F	P	F	P	F	P
TM1 (450-520)	1.3143	0.2588	1.0354	0.8854	1.3129	0.2607	1.0162	0.9468
TM2 (520- 600)	1.2350	0.3502	1.0148	0.9482	1.2624	0.3024	1.0081	0.9716
TM3 (630- 690)	1.1163	0.6741	1.0179	0.9460	1.2064	0.4733	1.0211	0.9363
TM4 (769- 900)	1.1604	0.3975	1.0764	0.6753	1.2936	0.1435	1.0664	0.7148
AVHRR1 (580- 680)	1.1360	0.5269	1.0002	0.9991	1.2051	0.3548	1.0126	0.9503
AVHRR2 (725-1100)	1.1425	0.1982	1.4199	0.0007	1.0833	0.4393	1.0612	0.5659

Figure A5. The spectral hemispherical reflectance (ρ) {lower curve} and spectral hemispherical transmittance(τ) {upper curve} of dicot leaf 5 (*Eucalyptus maniflora*). (a) The upper leaf surface irradiated with beam light, (b) the upper leaf surface irradiated with diffuse light, (c) the lower leaf surface irradiated with beam light and (d) the lower leaf surface irradiated with diffuse light.

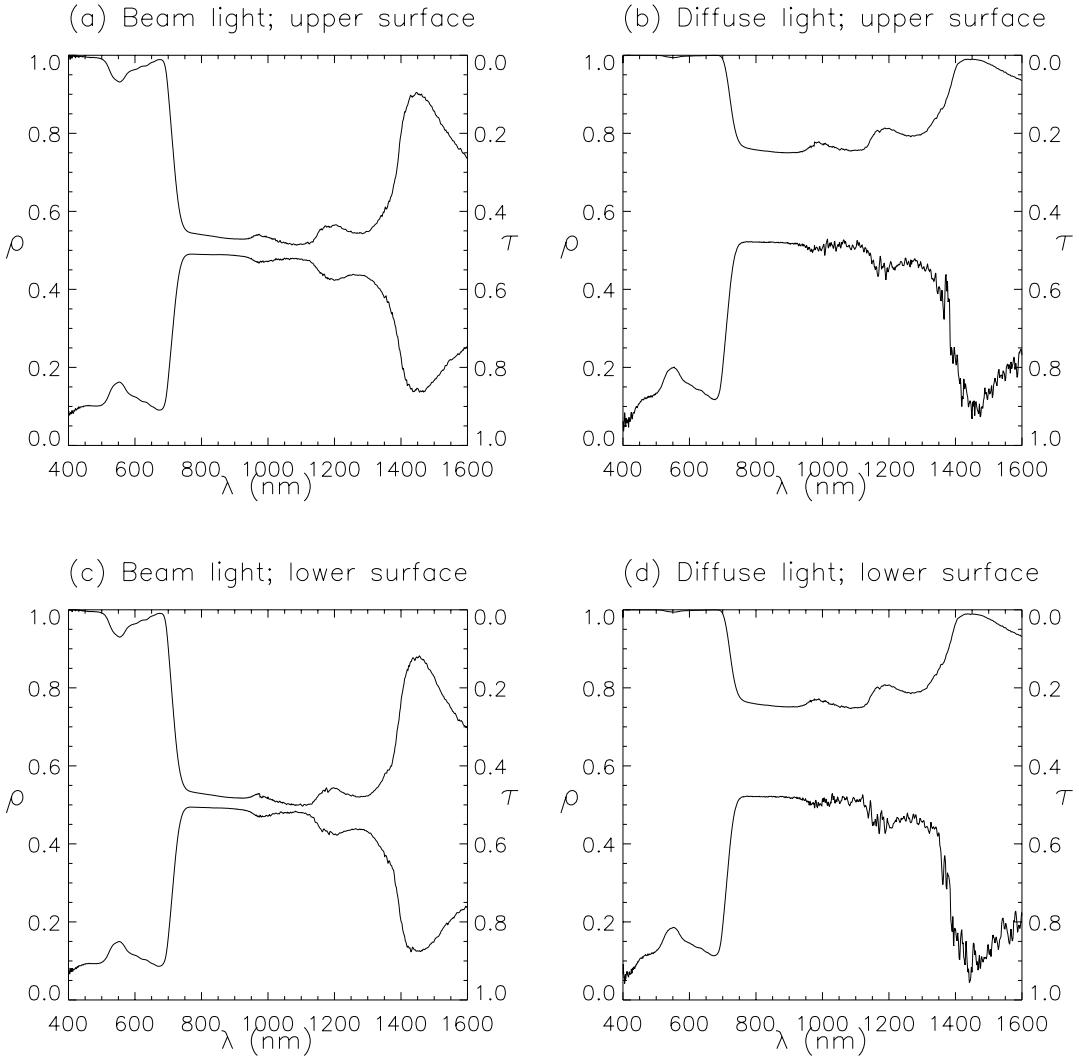

Table A5. Comparing the top and bottom surfaces of dicot leaf 5 (*Eucalyptus maniflora*). The F-variance statistic (F) and the probability (P) that the spectra of the top and bottom surfaces have significantly different variances are shown.

Band (Wavelength)	Beam Light				Diffuse Light			
	ρ		τ		ρ		τ	
	F	P	F	P	F	P	F	P
TM1 (450-520)	1.0718	0.7742	1.0592	0.8120	1.0671	0.7882	1.0020	0.9935
TM2 (520- 600)	1.1615	0.5075	1.1330	0.5804	1.1653	0.4981	1.0256	0.9107
TM3 (630- 690)	1.5294	0.1055	1.0335	0.8996	1.4990	0.1229	1.0121	0.9634
TM4 (769- 900)	2.4577	0.0000	1.0084	0.9620	1.4762	0.0272	1.0010	0.9957
AVHRR1 (580- 680)	1.3965	0.0982	1.1234	0.5639	1.3793	0.1113	1.0158	0.9382
AVHRR2 (725-1100)	1.1822	0.1060	1.1208	0.2707	1.1068	0.3268	1.0107	0.9184

Figure A6. The spectral hemispherical reflectance (ρ) {lower curve} and spectral hemispherical transmittance(τ) {upper curve} of dicot leaf 6 (*Eucalyptus maniflora* juvenile). (a) The upper leaf surface irradiated with beam light, (b) the upper leaf surface irradiated with diffuse light, (c) the lower leaf surface irradiated with beam light and (d) the lower leaf surface irradiated with diffuse light.

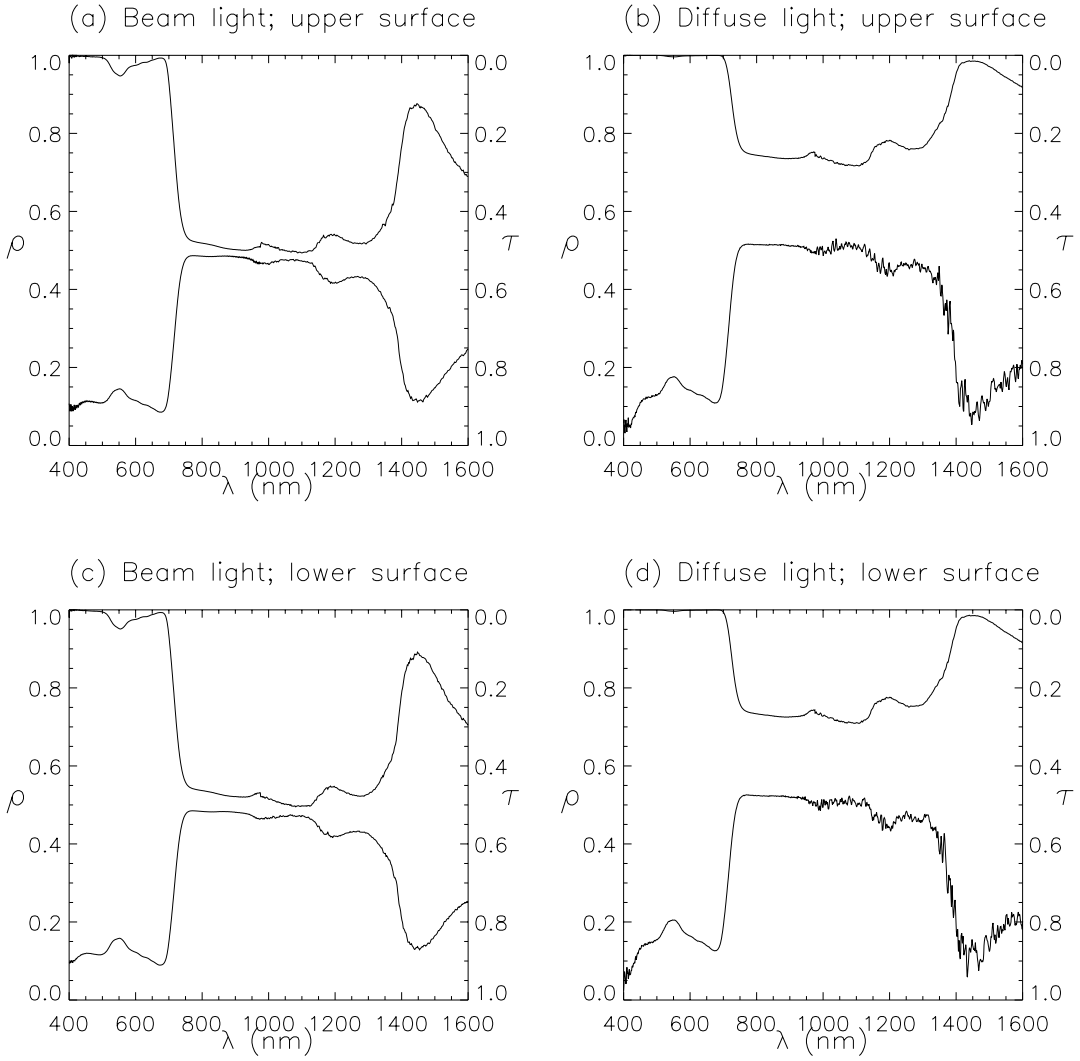

Table A6. Comparing the top and bottom surfaces of dicot leaf 6 (*Eucalyptus maniflora* juvenile). The F-variance statistic (F) and the probability (P) that the spectra of the top and bottom surfaces have significantly different variances are shown.

Band (Wavelength)	Beam Light				Diffuse Light			
	ρ		τ		ρ		τ	
	F	P	F	P	F	P	F	P
TM1 (450-520)	2.1183	0.0021	1.2025	0.4458	1.5624	0.0659	1.2935	0.2875
TM2 (520- 600)	1.4149	0.1251	1.1964	0.4273	1.3775	0.1568	1.0645	0.7820
TM3 (630- 690)	1.0906	0.7403	1.0656	0.8079	1.2419	0.4078	1.2894	0.3316
TM4 (769- 900)	1.4638	0.0307	1.1095	0.5546	1.6411	0.0050	1.0584	0.7466
AVHRR1 (580- 680)	1.3031	0.1896	1.1521	0.4825	1.4076	0.0905	1.2070	0.3510
AVHRR2 (725-1100)	1.1287	0.2421	1.2123	0.0630	1.0927	0.3917	1.0097	0.9260

Figure A7. The spectral hemispherical reflectance (ρ) {lower curve} and spectral hemispherical transmittance(τ) {upper curve} of dicot leaf 7 (*Eucalyptus polyanthemos*). (a) The upper leaf surface irradiated with beam light, (b) the upper leaf surface irradiated with diffuse light, (c) the lower leaf surface irradiated with beam light and (d) the lower leaf surface irradiated with diffuse light.

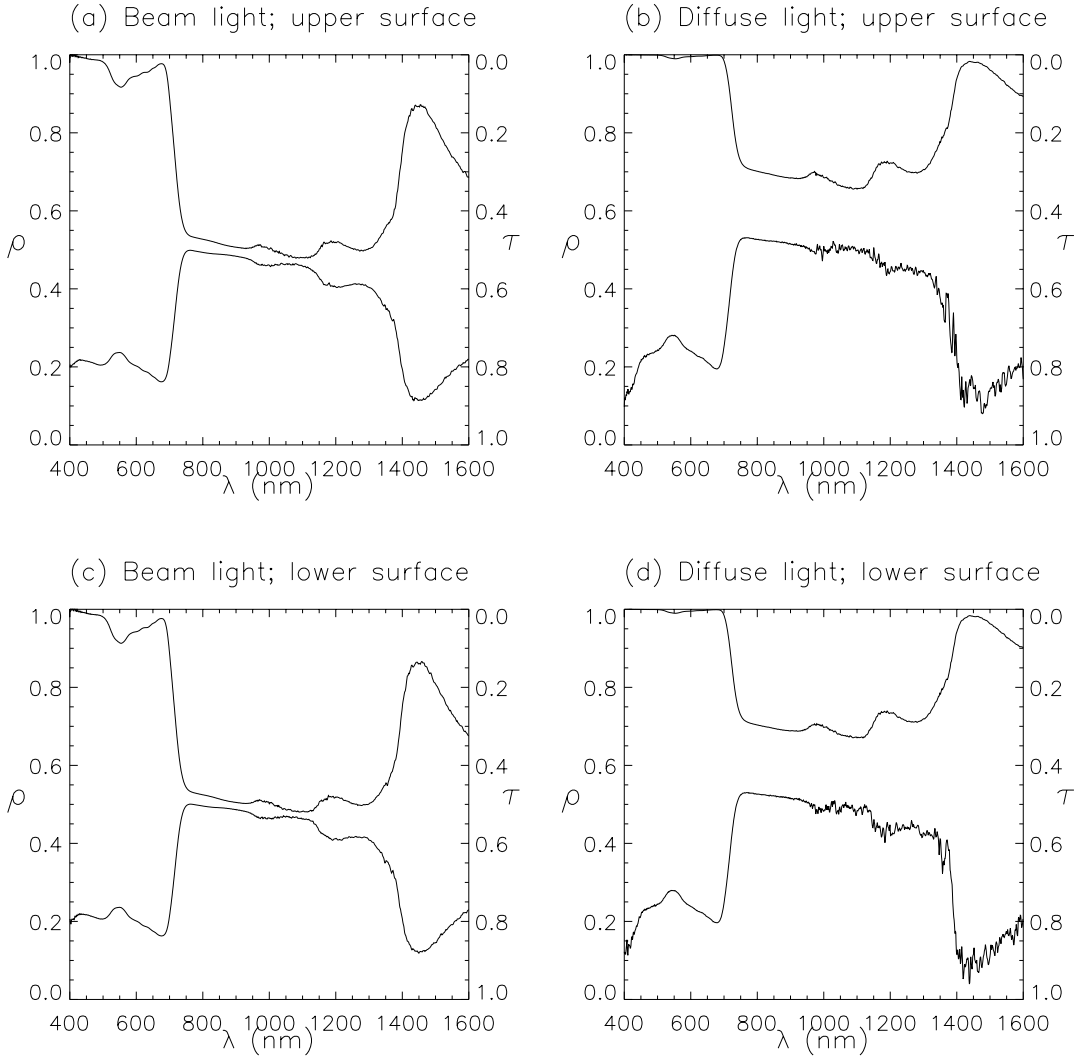

Table A7. Comparing the top and bottom surfaces of dicot leaf 7 (*Eucalyptus polyanthemos*). The F-variance statistic (F) and the probability (P) that the spectra of the top and bottom surfaces have significantly different variances are shown.

Band (Wavelength)	Beam Light				Diffuse Light			
	ρ		τ		ρ		τ	
	F	P	F	P	F	P	F	P
TM1 (450-520)	1.0286	0.9070	1.0944	0.7091	1.2310	0.3901	1.0547	0.8257
TM2 (520- 600)	1.0171	0.9400	1.0873	0.7109	1.0011	0.9962	1.0019	0.9932
TM3 (630- 690)	1.1890	0.5083	1.1097	0.6906	1.2097	0.4668	1.0188	0.9433
TM4 (769- 900)	1.1220	0.5127	1.0644	0.7227	1.1142	0.5384	1.2323	0.2351
AVHRR1 (580- 680)	1.0963	0.6481	1.1336	0.5338	1.1370	0.5241	1.0109	0.9572
AVHRR2 (725-1100)	1.0483	0.6487	1.0884	0.4129	1.5698	0.0000	1.2637	0.0239

Figure A8. The spectral hemispherical reflectance (ρ) {lower curve} and spectral hemispherical transmittance(τ) {upper curve} of dicot leaf 8 (*Eucalyptus dives*). (a) The upper leaf surface irradiated with beam light, (b) the upper leaf surface irradiated with diffuse light, (c) the lower leaf surface irradiated with beam light and (d) the lower leaf surface irradiated with diffuse light.

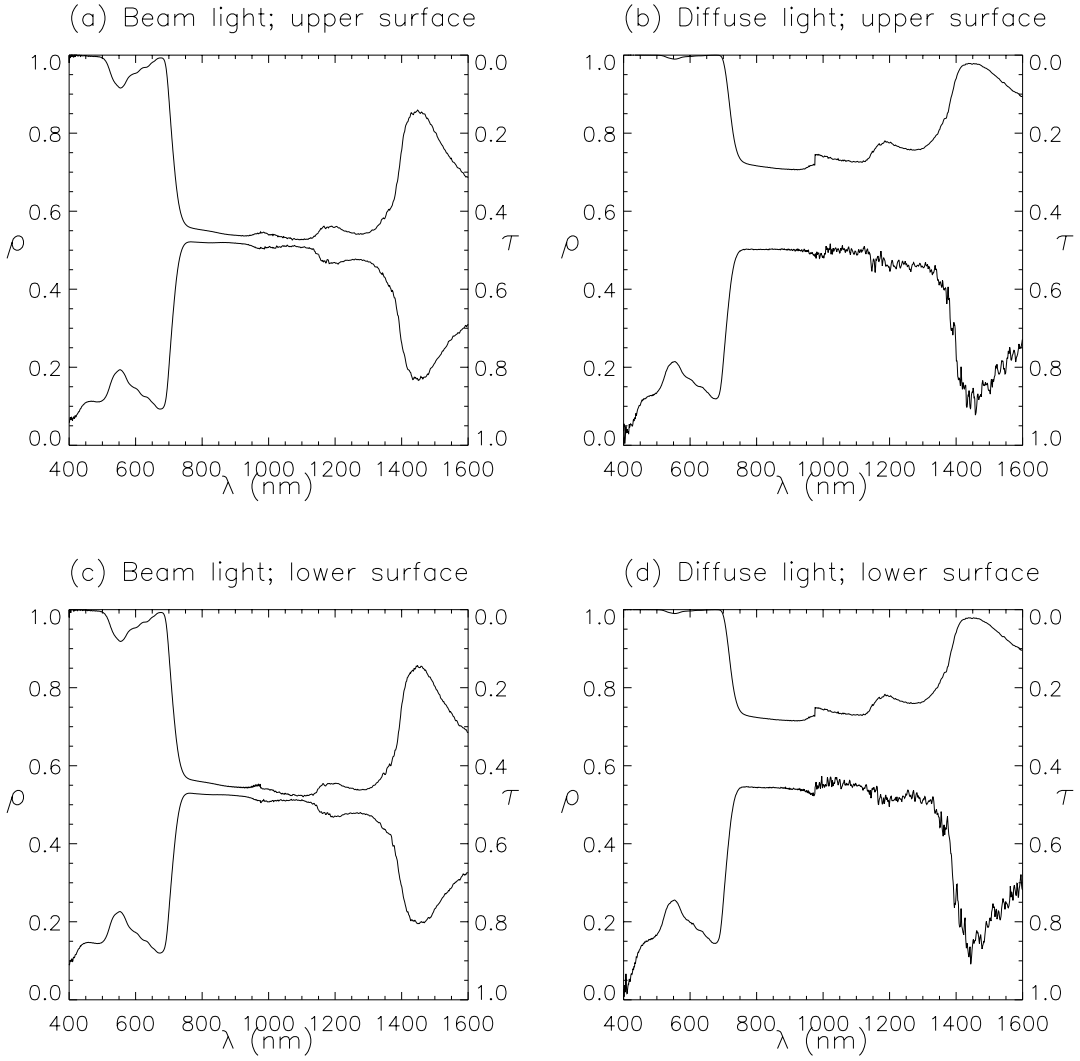

Table A8. Comparing the top and bottom surfaces of dicot leaf 8 (*Eucalyptus dives*). The F-variance statistic (F) and the probability (P) that the spectra of the top and bottom surfaces have significantly different variances are shown.

Band (Wavelength)	Beam Light				Diffuse Light			
	ρ		τ		ρ		τ	
	F	P	F	P	F	P	F	P
TM (450-520)	1.1800	0.4936	1.1681	0.5204	1.5304	0.0793	1.0562	0.8211
TM2 (520- 600)	1.2033	0.4126	1.0870	0.7118	1.4449	0.1040	1.0606	0.7943
TM3 (630- 690)	1.1160	0.6748	1.0260	0.9218	1.0239	0.9279	1.0409	0.8781
TM4 (769- 900)	3.6649	0.0000	1.0256	0.8854	4.4680	0.0000	1.2649	0.1817
AVHRR1 (580- 680)	1.0595	0.7741	1.0394	0.8478	1.2911	0.2055	1.0592	0.7754
AVHRR2 (725-1100)	1.0200	0.8483	1.2835	0.0160	1.4701	0.0002	1.1695	0.1305

Figure A9. The spectral hemispherical reflectance (ρ) {lower curve} and spectral hemispherical transmittance(τ) {upper curve} of dicot leaf 9 (*Eucalyptus pauciflora*). (a) The upper leaf surface irradiated with beam light, (b) the upper leaf surface irradiated with diffuse light, (c) the lower leaf surface irradiated with beam light and (d) the lower leaf surface irradiated with diffuse light.

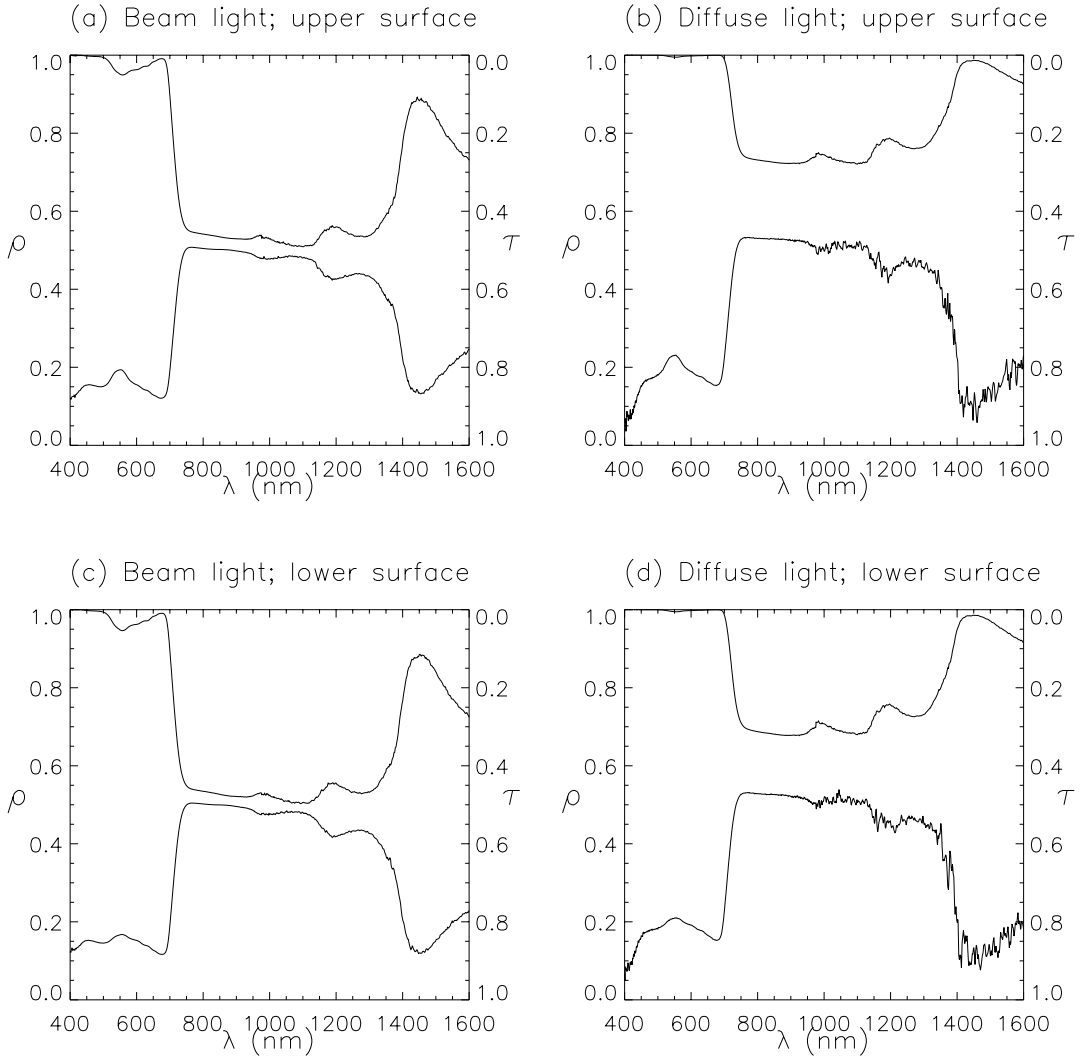

Table A9. Comparing the top and bottom surfaces of dicot leaf 9 (*Eucalyptus pauciflora*). The F-variance statistic (F) and the probability (P) that the spectra of the top and bottom surfaces have significantly different variances are shown.

Band (Wavelength)	Beam Light				Diffuse Light			
	ρ		τ		ρ		τ	
	F	P	F	P	F	P	F	P
TM1 (450-520)	1.9624	0.0057	1.1193	0.6409	2.4357	0.0003	1.0324	0.8951
TM2 (520- 600)	6.2904	0.0000	1.1427	0.5548	5.2066	0.0000	1.0159	0.9442
TM3 (630- 690)	1.3133	0.2980	1.0016	0.9953	1.3462	0.2564	1.3477	0.2547
TM4 (769- 900)	1.0566	0.7539	1.1851	0.3341	1.7201	0.0022	1.2582	0.1918
AVHRR1 (580- 680)	1.0901	0.6687	1.0295	0.8854	1.0198	0.9223	1.3126	0.1778
AVHRR2 (725-1100)	1.0892	0.4090	1.0170	0.8707	1.3202	0.0074	1.2837	0.0159

Figure A10. The spectral hemispherical reflectance (ρ) {lower curve} and spectral hemispherical transmittance(τ) {upper curve} of monocot leaf 1 (*Angiozanteos flavidius*). (a) The upper leaf surface irradiated with beam light, (b) the upper leaf surface irradiated with diffuse light, (c) the lower leaf surface irradiated with beam light and (d) the lower leaf surface irradiated with diffuse light.

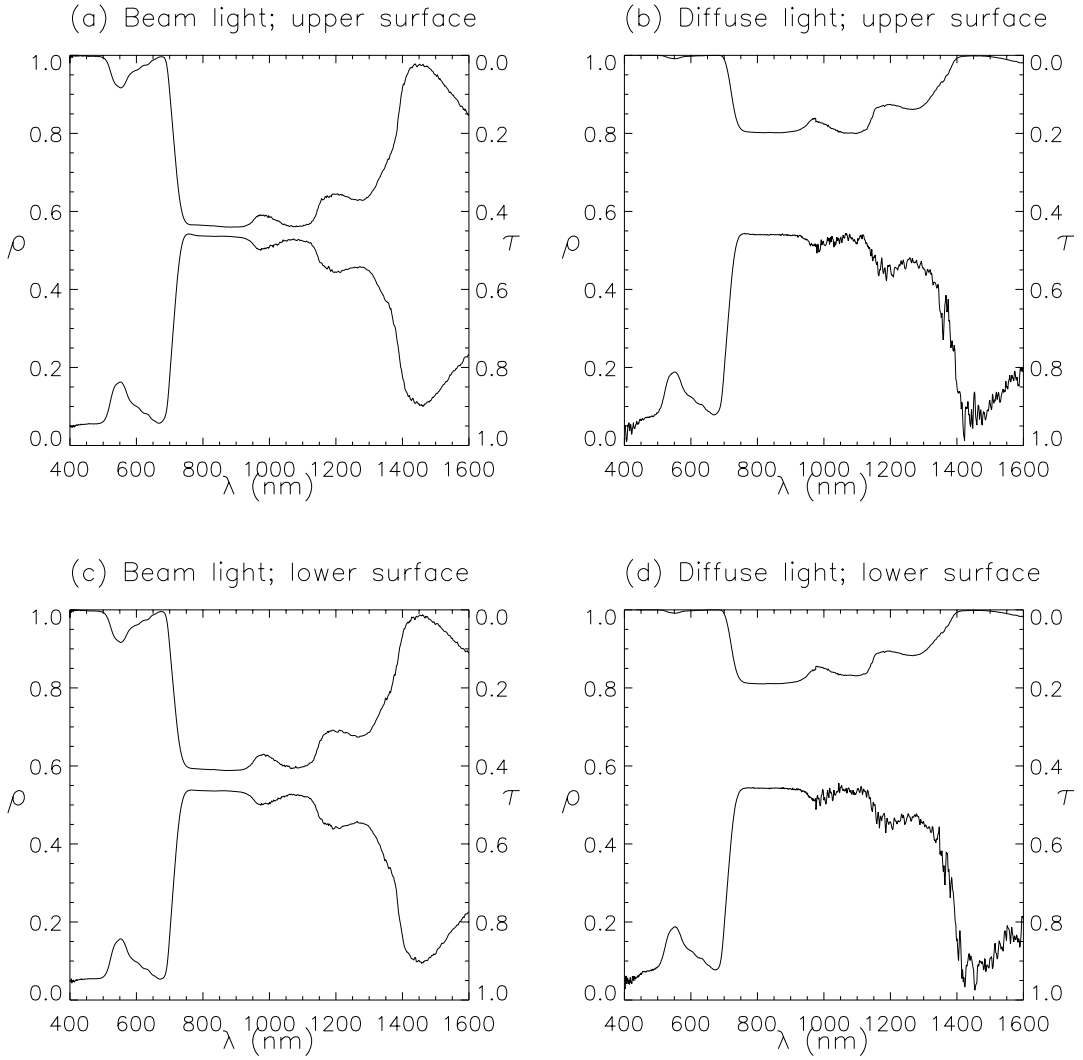

Table A10. Comparing the top and bottom surfaces of monocot leaf 1 (*Angiozanteos flavidius*). The F-variance statistic (F) and the probability (P) that the spectra of the top and bottom surfaces have significantly different variances are shown.

Band (Wavelength)	Beam Light				Diffuse Light			
	ρ		τ		ρ		τ	
	F	P	F	P	F	P	F	P
TM1 (450-520)	1.4410	0.1316	1.0614	0.8051	1.2730	0.3184	1.0089	0.9709
TM2 (520- 600)	1.1249	0.6021	1.0528	0.8196	1.0810	0.7300	1.0450	0.8454
TM3 (630- 690)	1.0783	0.7733	1.0384	0.8853	1.2597	0.3778	1.0564	0.8339
TM4 (769- 900)	2.2912	0.0000	1.6727	0.0036	1.4628	0.0310	1.2159	0.2665
AVHRR1 (580- 680)	1.0107	0.9579	1.0166	0.9347	1.0838	0.6898	1.0262	0.8981
AVHRR2 (725-1100)	1.1660	0.1381	1.1030	0.3436	1.1357	0.2190	1.3247	0.0067

Figure A11. The spectral hemispherical reflectance (ρ) {lower curve} and spectral hemispherical transmittance(τ) {upper curve} of monocot leaf 2 (*Ixia maculacata*). (a) The upper leaf surface irradiated with beam light, (b) the upper leaf surface irradiated with diffuse light, (c) the lower leaf surface irradiated with beam light and (d) the lower leaf surface irradiated with diffuse light.

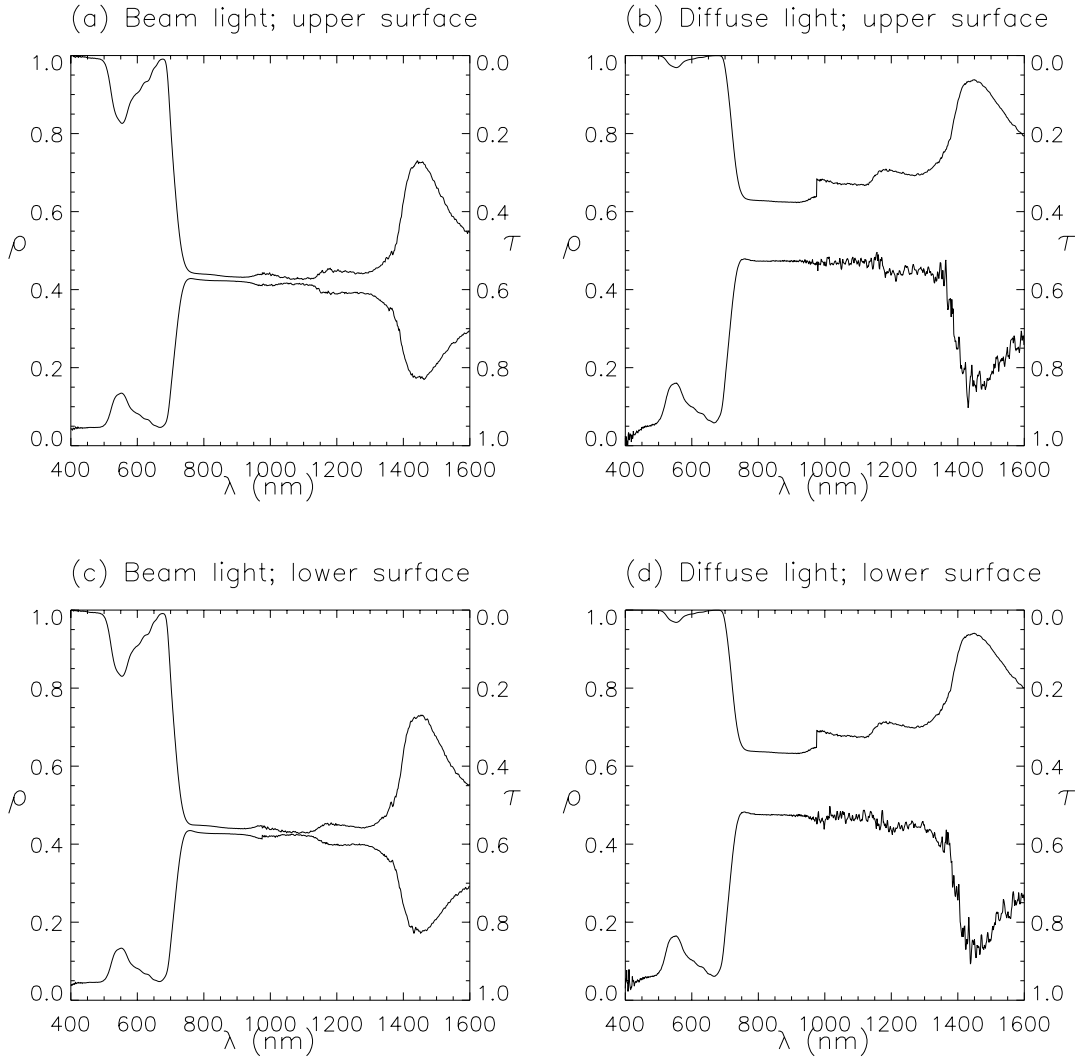

Table A11. Comparing the top and bottom surfaces of monocot leaf 2 (*Ixia maculacata*). The F-variance statistic (F) and the probability (P) that the spectra of the top and bottom surfaces have significantly different variances are shown.

Band (Wavelength)	Beam Light				Diffuse Light			
	ρ		τ		ρ		τ	
	F	P	F	P	F	P	F	P
TM1 (450-520)	1.0152	0.9503	1.0114	0.9625	1.1564	0.5477	1.2647	0.3317
TM2 (520- 600)	1.0014	0.9949	1.0008	0.9973	1.0210	0.9266	1.0005	0.9981
TM3 (630- 690)	1.0221	0.9334	1.1232	0.6569	1.0053	0.9838	1.2476	0.3980
TM4 (769- 900)	1.1198	0.5199	1.0279	0.8755	1.9655	0.0001	1.0481	0.7892
AVHRR1 (580- 680)	1.1079	0.6111	1.0834	0.6909	1.0566	0.7846	1.1018	0.6304
AVHRR2 (725-1100)	1.0989	0.3623	1.0161	0.8775	1.1362	0.2175	1.0770	0.4738

Figure A12. The spectral hemispherical reflectance (ρ) {lower curve} and spectral hemispherical transmittance(τ) {upper curve} of monocot leaf 3 (iris, bare rooted). (a) The upper leaf surface irradiated with beam light, (b) the upper leaf surface irradiated with diffuse light, (c) the lower leaf surface irradiated with beam light and (d) the lower leaf surface irradiated with diffuse light.

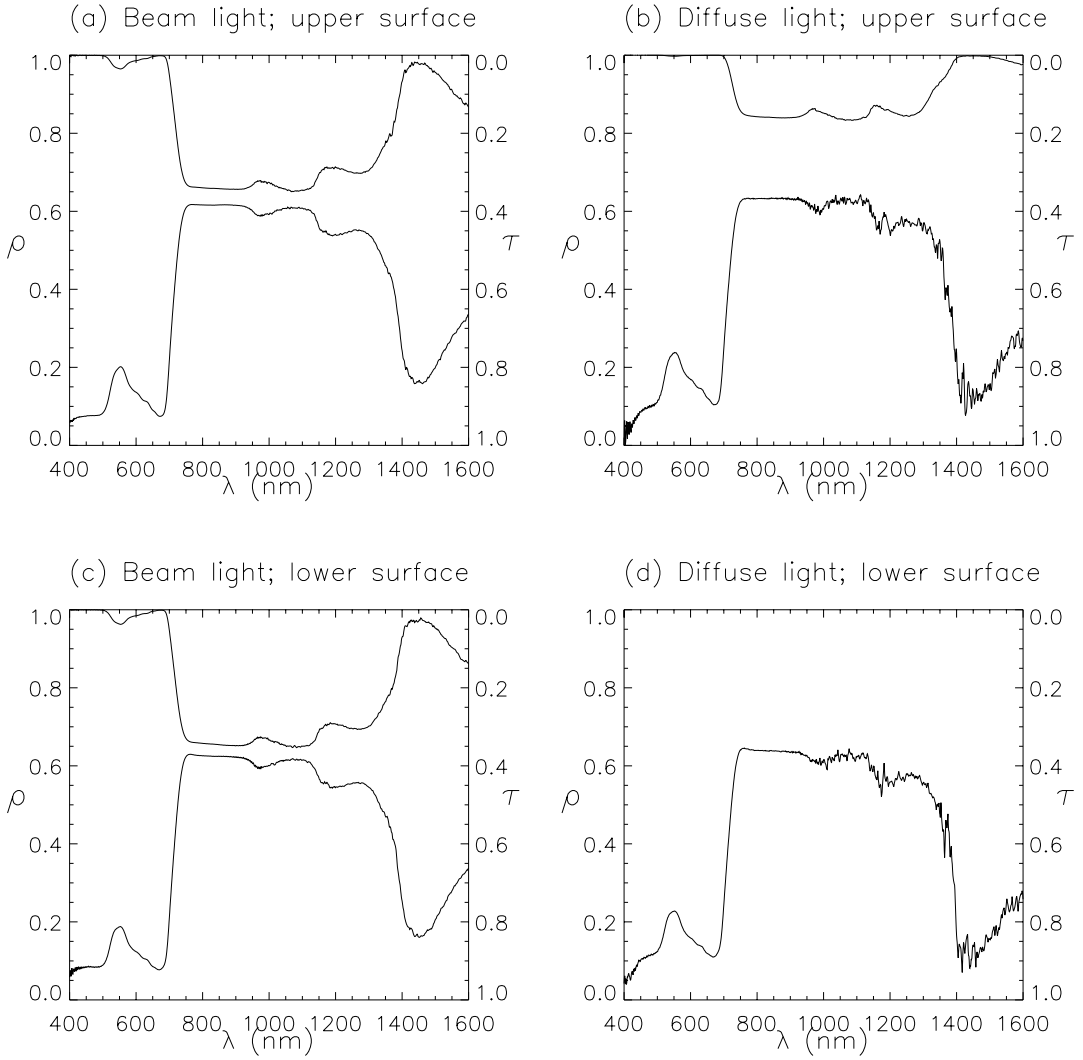

Table A12. Comparing the top and bottom surfaces of monocot leaf 3 (iris, bare rooted). The F-variance statistic (F) and the probability (P) that the spectra of the top and bottom surfaces have significantly different variances are shown.

Band (Wavelength)	Beam Light				Diffuse Light			
	ρ		τ		ρ		τ	
	F	P	F	P	F	P	F	P
TM1 (450-520)	1.3609	0.2031	1.0617	0.8044	1.3497	0.2154	******	******
TM2 (520- 600)	1.0697	0.7654	1.0872	0.7112	1.0269	0.9062	******	******
TM3 (630- 690)	2.0486	0.0066	1.3163	0.2939	2.0835	0.0055	******	******
TM4 (769- 900)	10.604	4 0.000	2.1468	0.0000	5.5629	0.0000	******	******
AVHRR1 (580- 680)	1.6032	0.0197	1.2195	0.3252	1.6053	0.0194	******	******
AVHRR2 (725-1100)	1.0404	0.7020	1.0194	0.8526	1.0131	0.8996	******	******

Note: ****** denotes missing data

Figure A13. The spectral hemispherical reflectance (ρ) {lower curve} and spectral hemispherical transmittance(τ) {upper curve} of monocot leaf 4 (iris, potted). (a) The upper leaf surface irradiated with beam light, (b) the upper leaf surface irradiated with diffuse light, (c) the lower leaf surface irradiated with beam light and (d) the lower leaf surface irradiated with diffuse light.

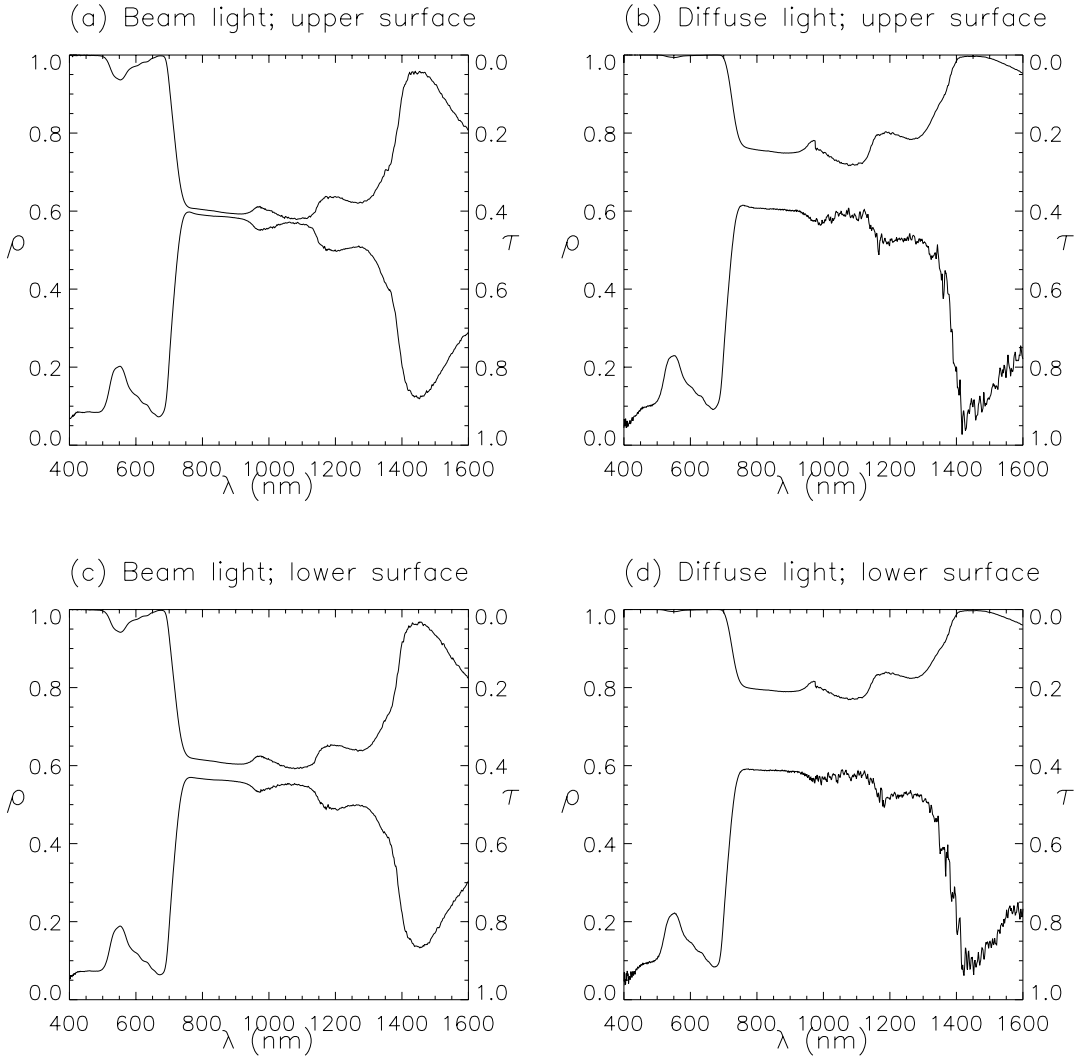

Table A13. Comparing the top and bottom surfaces of monocot leaf 4 (iris, potted). The F-variance statistic (F) and the probability (P) that the spectra of the top and bottom surfaces have significantly different variances are shown.

Band (Wavelength)	Beam Light				Diffuse Light			
	ρ		τ		ρ		τ	
	F	P	F	P	F	P	F	P
TM1 (450-520)	1.2926	0.2888	1.2283	0.3953	1.2548	0.3481	******	******
TM2 (520- 600)	1.1938	0.4328	1.1813	0.4607	1.1370	0.5696	1.3393	0.1964
TM3 (630- 690)	1.0927	0.7348	1.2532	0.3885	1.2188	0.4495	1.4813	0.1342
TM4 (769- 900)	1.4257	0.0441	1.0282	0.8744	2.5466	0.0000	1.6878	0.0031
AVHRR1 (580- 680)	1.0146	0.9429	1.2358	0.2938	1.0785	0.7075	1.4080	0.0903
AVHRR2 (725-1100)	1.1223	0.2650	1.0338	0.7484	1.0333	0.7515	1.6897	0.0000

Note: ****** denotes missing data

Figure A14. The spectral hemispherical reflectance (ρ) {lower curve} and spectral hemispherical transmittance(τ) {upper curve} of monocot leaf 5 (*Gladiolus .spp*). (a) The upper leaf surface irradiated with beam light, (b) the upper leaf surface irradiated with diffuse light, (c) the lower leaf surface irradiated with beam light and (d) the lower leaf surface irradiated with diffuse light.

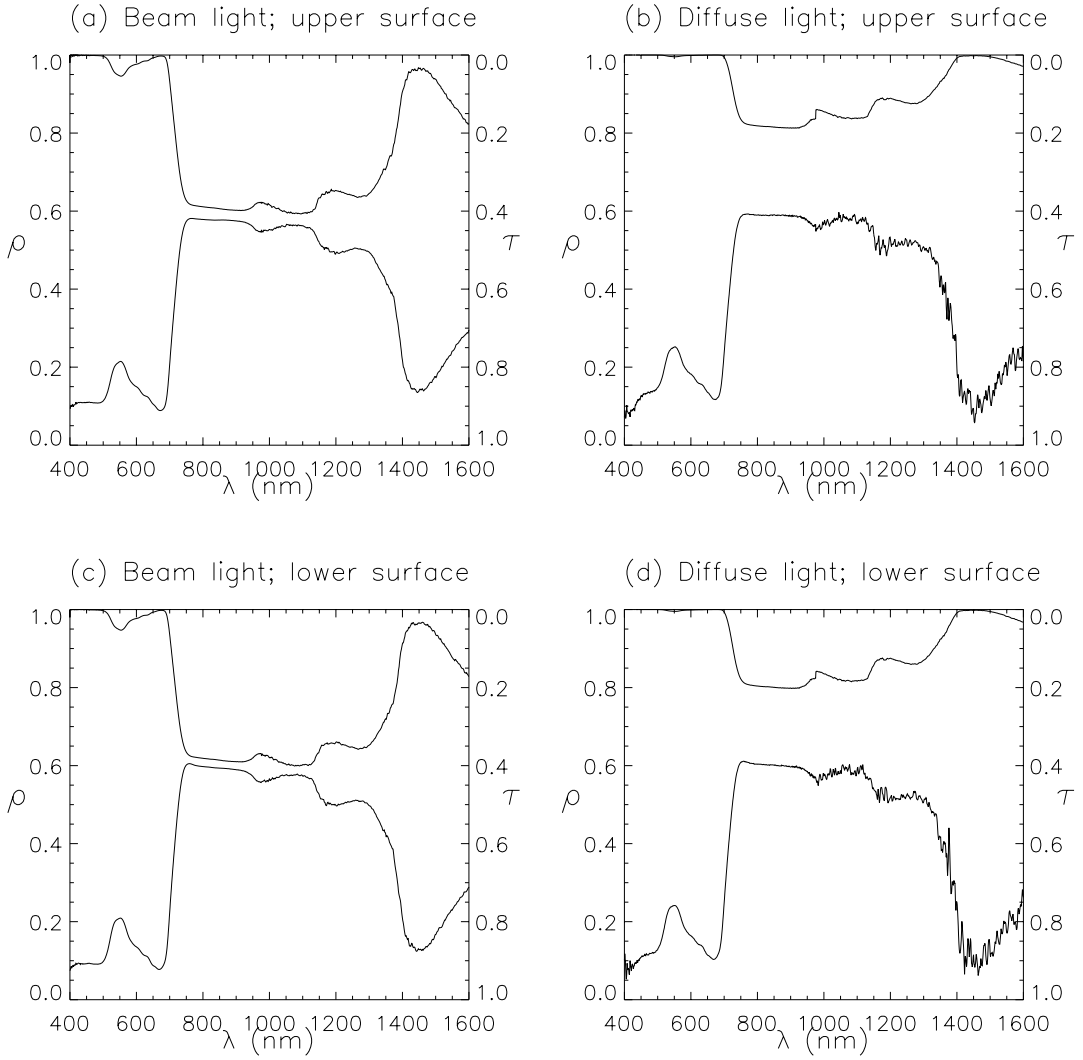

Table A14. Comparing the top and bottom surfaces of monocot leaf 5 (*Gladiolus .spp*). The F-variance statistic (F) and the probability (P) that the spectra of the top and bottom surfaces have significantly different variances are shown.

Band (Wavelength)	Beam Light				Diffuse Light			
	ρ		τ		ρ		τ	
	F	P	F	P	F	P	F	P
TM1 (450-520)	1.4238	0.1447	1.0470	0.8493	1.1595	0.5405	1.0100	0.9673
TM2 (520- 600)	1.3074	0.2358	1.0459	0.8424	1.2686	0.2925	1.1441	0.5511
TM3 (630- 690)	1.1636	0.5624	1.0067	0.9795	1.2237	0.4405	1.0087	0.9736
TM4 (769- 900)	5.1662	0.0000	1.0631	0.7278	5.5523	0.0000	1.0735	0.6865
AVHRR1 (580- 680)	1.0105	0.9588	1.0296	0.8848	1.0468	0.8205	1.0710	0.7336
AVHRR2 (725-1100)	1.0266	0.7997	1.0164	0.8750	1.0096	0.9262	1.0435	0.6807

Figure A15. The spectral hemispherical reflectance (ρ) {lower curve} and spectral hemispherical transmittance(τ) {upper curve} of monocot leaf 6 *(Hippiastrum*). (a) The upper leaf surface irradiated with beam light, (b) the upper leaf surface irradiated with diffuse light, (c) the lower leaf surface irradiated with beam light and (d) the lower leaf surface irradiated with diffuse light.

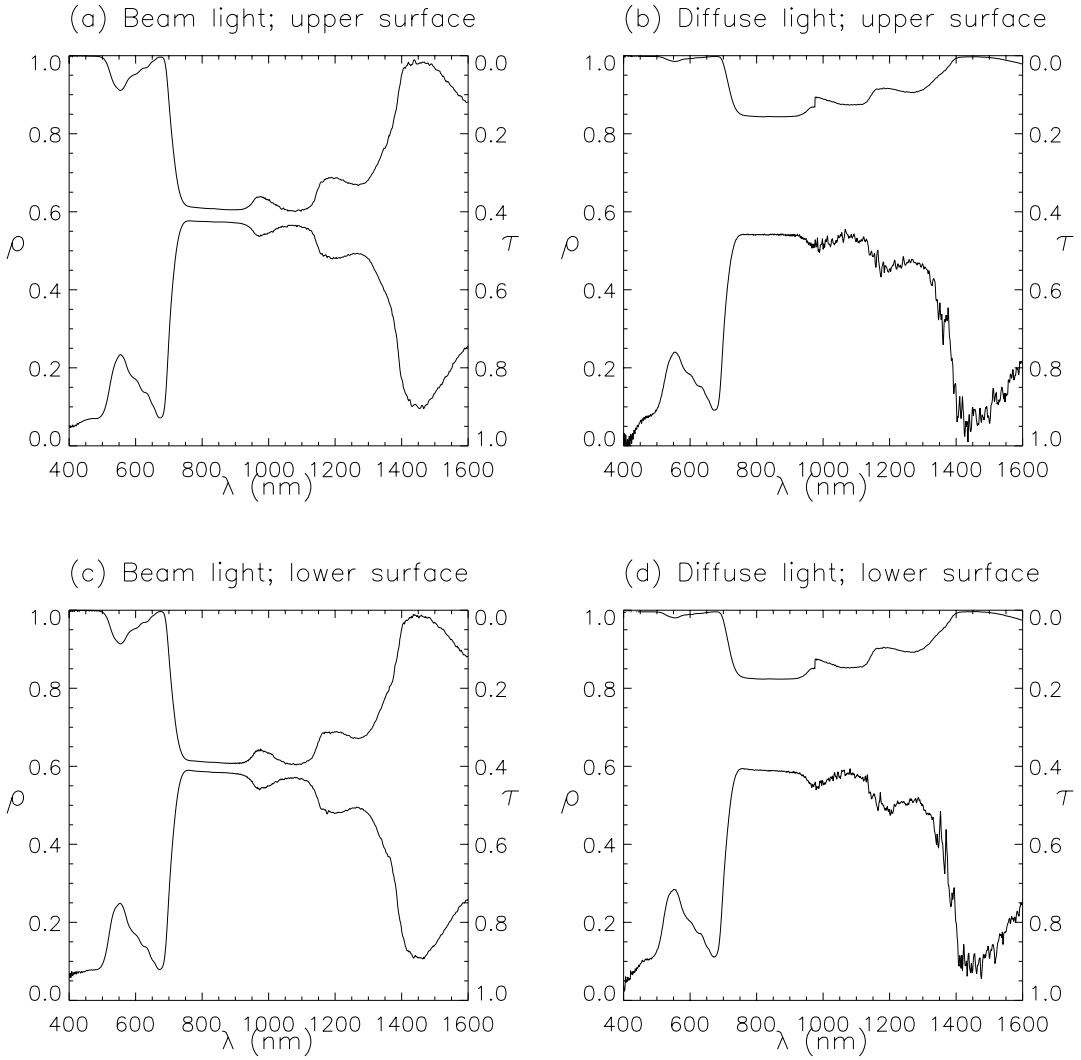

Table A15. Comparing the top and bottom surfaces of monocot leaf 6 (*Hippiastrum*). The F-variance statistic (F) and the probability (P) that the spectra of the top and bottom surfaces have significantly different variances are shown.

Band (Wavelength)	Beam Light				Diffuse Light			
	ρ		τ		ρ		τ	
	F	P	F	P	F	P	F	P
TM1 (450-520)	1.5646	0.0651	1.1008	0.6912	1.4793	0.1062	1.5867	0.0572
TM2 (520- 600)	1.2389	0.3430	1.0811	0.7297	1.4704	0.0886	1.3682	0.1657
TM3 (630- 690)	1.3755	0.2237	1.0144	0.9565	1.1354	0.6274	1.7873	0.0274
TM4 (769- 900)	2.9314	0.0000	1.0897	0.6252	5.2492	0.0000	1.3104	0.1245
AVHRR1 (580- 680)	1.1128	0.5960	1.0269	0.8951	1.1093	0.6068	1.6132	0.0182
AVHRR2 (725-1100)	1.4451	0.0004	1.0232	0.8249	1.3889	0.0015	1.0024	0.9813

Figure A16. The spectral hemispherical reflectance (ρ) {lower curve} and spectral hemispherical transmittance(τ) {upper curve} of monocot leaf (*Billbergia nutans*). (a) The upper leaf surface irradiated with beam light, (b) the upper leaf surface irradiated with diffuse light, (c) the lower leaf surface irradiated with beam light and (d) the lower leaf surface irradiated with diffuse light.

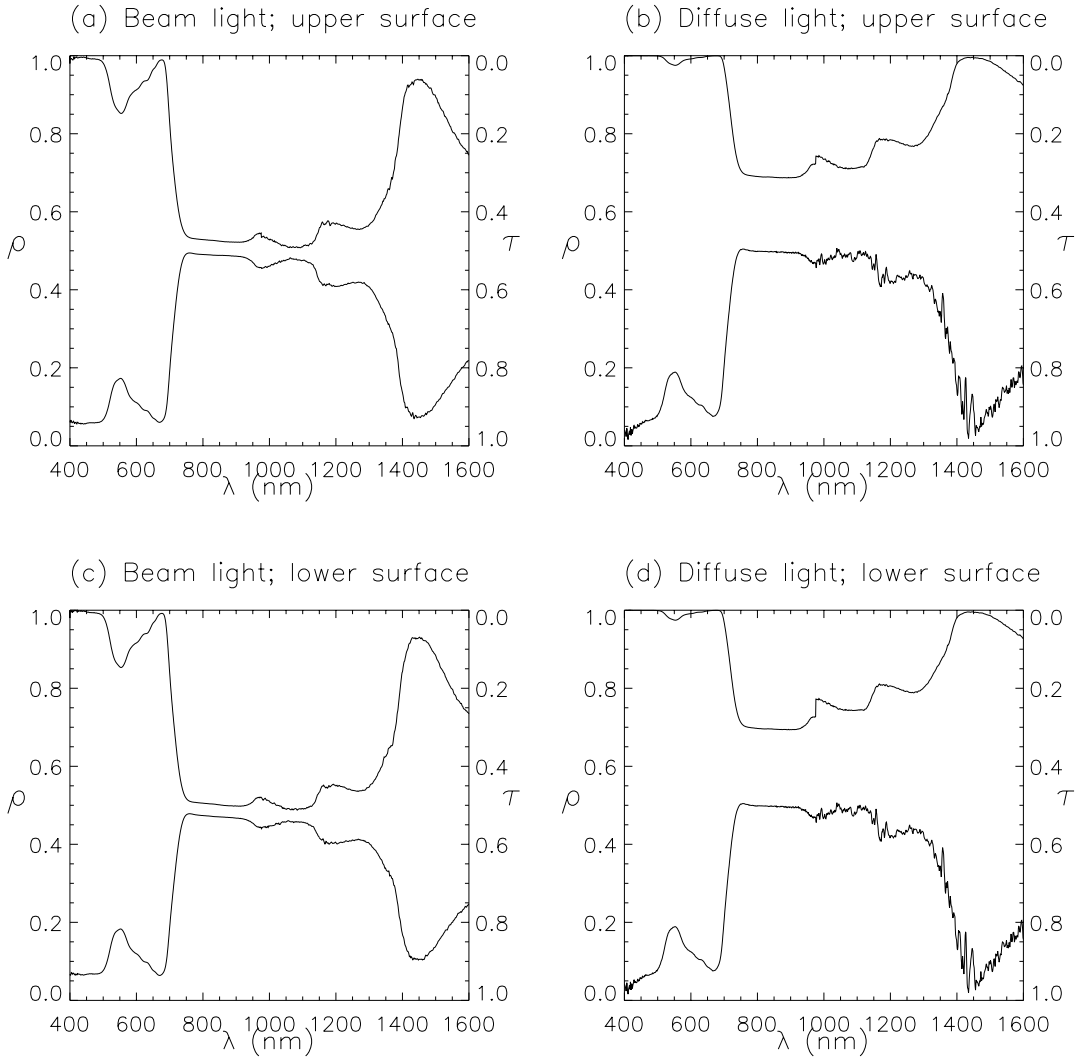

Table A16. Comparing the top and bottom surfaces of monocot leaf 6 (*Billbergia nutans*) The F-variance statistic (F) and the probability (P) that the spectra of the top and bottom surfaces have significantly different variances are shown.

Band (Wavelength)	Beam Light				Diffuse Light			
	ρ		τ		ρ		τ	
	F	P	F	P	F	P	F	P
TM1 (450-520)	1.1476	0.5690	1.0284	0.9077	1.1564	0.5477	1.1323	0.6072
TM2 (520- 600)	1.0267	0.9072	1.0794	0.7351	1.0121	0.9574	1.0456	0.8434
TM3 (630- 690)	1.2297	0.4294	1.0499	0.8522	1.4098	0.1901	1.1673	0.5543
TM4 (769- 900)	2.1439	0.0000	1.1632	0.3900	1.2554	0.1961	1.1423	0.4494
AVHRR1 (580- 680)	1.2007	0.3645	1.0274	0.8935	1.3463	0.1407	1.1096	0.6060
AVHRR2 (725-1100)	1.0799	0.4574	1.2290	0.0465	1.2385	0.0390	1.8494	0.0000

Appendix B

This appendix contains the T test summary tables. These tests are of differences between the hemispherical reflectance and hemispherical transmittance of beam and diffuse light in satellite equivalent bandwidths. For each test the tables show the T statistic and the probability (P) of obtaining a higher value of T. The two means are significantly different if the P value is less than 0.05.

450 - 520(nm) waveband (Landsat Thematic Mapper Channel 1)

Table B1.1. T test of differences between the mean hemispherical reflectance (ρ) and hemispherical transmittance (τ) of the upper and lower surfaces of monocot and dicot leaves.

Leaf type	Beam				Diffuse			
	ρ		τ		ρ		τ	
	T	P	T	P	T	P	T	P
Monocot	0.0486	0.9620	0.1419	0.8900	-0.3758	0.7138	-0.5855	0.5802
Dicot	-0.1080	0.9153	0.0478	0.9625	-0.1480	0.8842	0.1168	0.9090

Table B1.2. T test of difference between the mean hemispherical reflectance (ρ) and hemispherical transmittance (τ) of monocot and dicot leaves.

Leaf surface	Beam				Diffuse			
	ρ		τ		ρ		τ	
	T	P	T	P	T	P	T	P
Top	-2.5431	0.0252*	0.2528	0.8054	-2.5815	0.0220*	1.4612	0.1988
Bottom	-2.7650	0.0181*	0.1363	0.8940	-2.4614	0.0290*	1.3852	0.2367

Table B1.3. T test of difference between the mean hemispherical reflectance (ρ) and hemispherical transmittance (τ) of beam and diffuse light.

Leaf surface	Monocot				Dicot			
	ρ		τ		ρ		τ	
	T	P	T	P	T	P	T	P
Top	-1.2361	0.2419	3.0540	0.0272*	-1.0851	0.2940	4.6247	0.0017*
Bottom	-1.9737	0.0741	2.7782	0.0425*	-1.0786	0.2968	4.9665	0.0025*

Table B1.4. T test of difference between the hemispherical transmittance of diffuse light by monocot and dicot leaves.

Leaf surface	T	P
Top	-0.2107	0.8403
Bottom	0.0591	0.9548

Note: These tables show the T statistic and the probability (P) of obtaining a higher value of T. The two means are significantly different if the P value is less than 0.05 and are marked *.

520 - 600(nm) waveband (Landsat Thematic Mapper Channel 2)

Table B2.1. T test of differences between the mean hemispherical reflectance (ρ) and hemispherical transmittance (τ) of the upper and lower surfaces of monocot and dicot leaves.

Leaf type	Beam				Diffuse			
	ρ		τ		ρ		τ	
	T	P	T	P	T	P	T	P
Monocot	0.1368	0.8935	0.0688	0.9463	-0.1543	0.8799	-0.1929	0.8510
Dicot	0.0571	0.9552	-0.1045	0.9181	-0.0105	0.9918	0.0811	0.9363

Table B2.2. T test of difference between the mean hemispherical reflectance (ρ) and hemispherical transmittance (τ) of monocot and dicot leaves.

Leaf surface	Beam				Diffuse			
	ρ		τ		ρ		τ	
	T	P	T	P	T	P	T	P
Top	0.4996	0.6251	1.5682	0.1601	0.0252	0.9802	1.7764	0.1207
Bottom	0.4091	0.6887	1.4664	0.1851	0.1574	0.8772	2.1725	0.0776

Table B2.3. T test of difference between the mean hemispherical reflectance (ρ) and hemispherical transmittance (τ) of beam and diffuse light.

Leaf surface	Monocot				Dicot			
	ρ		τ		ρ		τ	
	T	P	T	P	T	P	T	P
Top	-1.4278	0.1789	3.8849	0.0072*	-1.7904	0.0923	8.5300	0.0000*
Bottom	-1.5862	0.1390	3.9983	0.0088*	-1.7528	0.0989	8.8069	0.0000*

Table B2.4. T test of difference between the hemispherical transmittance of diffuse light by monocot and dicot leaves.

Leaf surface	T	P
Top	-1.9407	0.1006
Bottom	-1.7057	0.1392

Note: These tables show the T statistic and the probability (P) of obtaining a higher value of T. The two means are significantly different if the P value is less than 0.05 and are marked *.

630 - 690(nm)waveband (Landsat Thematic Mapper Channel 3)

Table B3.1. T test of differences between the mean hemispherical reflectance (ρ) and hemispherical transmittance (τ) of the upper and lower surfaces of monocot and dicot leaves.

Leaf type	Beam				Diffuse			
	ρ		τ		ρ		τ	
	T	P	T	P	T	P	T	P
Monocot	0.2698	0.7919	0.1275	0.9007	0.0489	0.9618	-0.4990	0.6315
Dicot	-0.0055	0.9957	-0.0529	0.9585	-0.0346	0.9728	0.0439	0.9655

Table B3.2. T test of difference between the mean hemispherical reflectance (ρ) and hemispherical transmittance (τ) of monocot and dicot leaves.

Leaf surface	Beam				Diffuse			
	ρ		τ		ρ		τ	
	T	P	T	P	T	P	T	P
Top	-2.1776	0.0483	-0.1393	0.8918	-2.4077	0.0306	0.7621	0.4677
Bottom	-2.4444	0.0301*	-0.3468	0.7350	-2.3436	0.0347	1.1631	0.2931

Table B3.3. T test of difference between the mean hemispherical reflectance (ρ) and hemispherical transmittance (τ) of beam and diffuse light.

Leaf surface	Monocot				Dicot			
	ρ		τ		ρ		τ	
	T	P	T	P	T	P	T	P
Top	-2.0608	0.0629	3.2575	0.0168*	-1.9294	0.0717	5.5002	0.0006*
Bottom	-2.2661	0.0452*	3.4284	0.0163*	-1.8755	0.0794	5.5116	0.0005*

Table B3.4. T test of difference between the hemispherical transmittance of diffuse light by monocot and dicot leaves.

Leaf surface	T	P
Top	-0.1276	0.9015
Bottom	0.2035	0.8432

Note: These tables show the T statistic and the probability (P) of obtaining a higher value of T. The two means are significantly different if the P value is less than 0.05 and are marked *.

769 - 900(nm)waveband (Landsat Thematic Mapper Channel 4)

Table B4.1. T test of differences between the mean hemispherical reflectance (ρ) and hemispherical transmittance (τ) of the upper and lower surfaces of monocot and dicot leaves.

Leaf type	Beam				Diffuse			
	ρ		τ		ρ		τ	
	T	P	T	P	T	P	T	P
Monocot	0.0031	0.9976	0.1077	0.9160	-0.0939	0.9268	0.1066	0.9173
Dicot	-0.4778	0.6396	-0.5741	0.5742	-0.6942	0.4983	-0.3601	0.7235

Table B4.2. T test of difference between the mean hemispherical reflectance (ρ) and hemispherical transmittance (τ) of monocot and dicot leaves.

Leaf surface	Beam				Diffuse			
	ρ		τ		ρ		τ	
	T	P	T	P	T	P	T	P
Top	1.9189	0.0966	-1.1263	0.2971	1.9848	0.0890	-0.9078	0.3934
Bottom	1.6791	0.1401	-1.4624	0.1892	1.6093	0.1511	-0.8382	0.4342

Table B4.3. T test of difference between the mean hemispherical reflectance (ρ) and hemispherical transmittance (τ) of beam and diffuse light.

Leaf surface	Monocot				Dicot			
	ρ		τ		ρ		τ	
	T	P	T	P	T	P	T	P
Top	-0.3261	0.7501	4.7303	0.0005*	-1.8081	0.0907	15.7176	0.0000*
Bottom	-0.3875	0.7052	4.6321	0.0009*	-1.9905	0.0652	17.0643	0.0000*

Table B4.4. T test of difference between the hemispherical transmittance of diffuse light by monocot and dicot leaves.

Leaf surface	T	P
Top	-0.0017	0.9987
Bottom	0.1302	0.8984

Note: These tables show the T statistic and the probability (P) of obtaining a higher value of T. The two means are significantly different if the P value is less than 0.05 and are marked *.

580 - 680(nm) waveband (AVHRR Channel 1)

Table B5.1. T test of differences between the mean hemispherical reflectance (ρ) and hemispherical transmittance (τ) of the upper and lower surfaces of monocot and dicot leaves.

Leaf type	Beam				Diffuse			
	ρ		τ		ρ		τ	
	T	P	T	P	T	P	T	P
Monocot	0.2851	0.7804	0.0915	0.9286	0.0337	0.9737	-0.3888	0.7064
Dicot	0.0171	0.9866	-0.0832	0.9347	-0.0245	0.9808	0.0810	0.9365

Table B5.2. T test of difference between the mean hemispherical reflectance (ρ) and hemispherical transmittance (τ) of monocot and dicot leaves.

Leaf surface	Beam				Diffuse			
	ρ		τ		ρ		τ	
	T	P	T	P	T	P	T	P
Top	-1.2805	0.2213	0.7795	0.4579	-1.6670	0.1178	1.4255	0.1945
Bottom	-1.5515	0.1437	0.6540	0.5305	-1.6440	0.1225	1.7622	0.1326

Table 5.3. T test of difference between the mean hemispherical reflectance (ρ) and hemispherical transmittance (τ) of beam and diffuse light.

Leaf surface	Monocot				Dicot			
	ρ		τ		ρ		τ	
	T	P	T	P	T	P	T	P
Top	-1.6328	0.1290	3.4611	0.0130*	-1.8606	0.0813	6.6758	0.0001*
Bottom	-1.9226	0.0799	3.6596	0.0133*	-1.8146	0.0886	6.7243	0.0001*

Table B5.4. T test of difference between the hemispherical transmittance of diffuse light by monocot and dicot leaves.

Leaf surface	T	P
Top	-1.0605	0.3262
Bottom	-0.8241	0.4375

Note: These tables show the T statistic and the probability (P) of obtaining a higher value of T. The two means are significantly different if the P value is less than 0.05 and are marked *.

725 - 1100(nm) waveband (AVHRR Channel 2)

Table B6.1. T test of differences between the mean hemispherical reflectance (ρ) and hemispherical transmittance (τ) of the upper and lower surfaces of monocot and dicot leaves.

Leaf type	Beam				Diffuse			
	ρ		τ		ρ		τ	
	T	P	T	P	T	P	T	P
Monocot	0.0104	0.9919	0.1187	0.9075	-0.0757	0.9409	0.1635	0.8735
Dicot	-0.4277	0.6750	-0.6063	0.5531	-0.7016	0.4948	-0.3908	0.7011

Table B6.2. T test of difference between the mean hemispherical reflectance (ρ) and hemispherical transmittance (τ) of monocot and dicot leaves.

Leaf surface	Beam				Diffuse			
	ρ		τ		ρ		τ	
	T	P	T	P	T	P	T	P
Top	1.9141	0.0970	-1.2807	0.2415	2.0363	0.0834	-1.0867	0.3111
Bottom	1.6961	0.1367	-1.6146	0.1531	1.6107	0.1500	-1.1689	0.2862

Table B6.3. T test of difference between the mean hemispherical reflectance (ρ) and hemispherical transmittance (τ) of beam and diffuse light.

Leaf surface	Monocot				Dicot			
	ρ		τ		ρ		τ	
	T	P	T	P	T	P	T	P
Top	-0.3883	0.7048	4.9928	0.0003*	-2.0170	0.0633	15.9532	0.0000*
Bottom	-0.4373	0.6697	4.9596	0.0006*	-2.1335	0.0503	17.9482	0.0000*

Table B6.4. T test of difference between the hemispherical transmittance of diffuse light by monocot and dicot leaves.

Leaf surface	T	P
Top	-0.0882	0.9322
Bottom	-0.1781	0.8614

Note: These tables show the T statistic and the probability (P) of obtaining a higher value of T. The two means are significantly different if the P value is less than 0.05 and are marked *.

CENTRE OFFICE

Department of Civil Engineering PO Box 60 Monash University VIC 3800 Australia
Telephone +61 3 9905 2704 Facsimile +61 3 9905 5033 Email crcch@eng.monash.edu.au www.catchment.crc.org.au

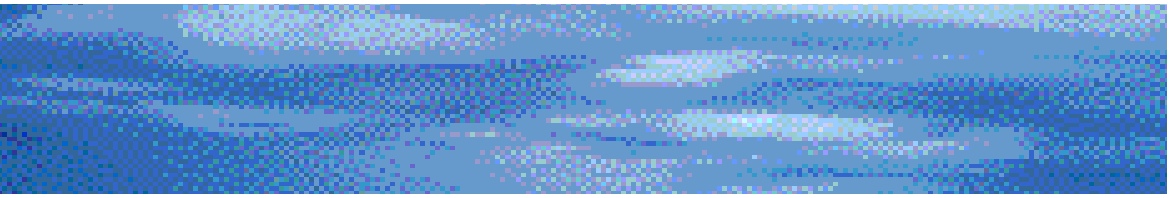

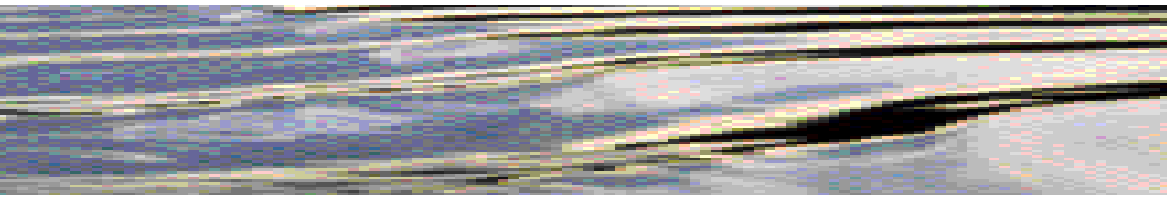

The Cooperative Research Centre for Catchment Hydrology is a cooperative venture formed under the Commonwealth CRC Program between:

- Brisbane City Council
- Bureau of Meteorology
- CSIRO Land and Water
- Department of Land and Water Conservation, NSW
- Department of Natural Resources and Environment, Vic
- Goulburn-Murray Water
- Griffith University
- Melbourne Water
- Monash University
- Murray-Darling Basin Commission
- Natural Resources and Mines, Qld
- Southern Rural Water
- The University of Melbourne
- Wimmera Mallee Water

Associates:

- SA Water
- State Forests of NSW

Established and supported under the Australian Government's Cooperative Research Centre Program